UNITED STATES NAVY

PROJECT SQUID

TECHNICAL REPORT NO. 9

COMPRESSIBLE FLOW THROUGH REED VALVES

FOR PULSE JET ENGINES.

I. RING REED VALVES

By

PAUL TORDA

I. P. VILLALBA

J. H. BRICK

JUNE, 1948

POLYTECHNIC INSTITUTE
OF BROOKLYN

TECHNICAL REPORT NO. 9

PROJECT SQUID

A COOPERATIVE PROGRAM
OF FUNDAMENTAL RESEARCH IN JET PROPULSION
for the
OFFICE OF NAVAL RESEARCH
of the
NAVY DEPARTMENT
CONTRACT N6-ORI-98, TASK ORDER II
NR 220-039

COMPRESSIBLE FLOW THROUGH REED VALVES FOR PULSE JET ENGINES. I. HINGED REED VALVES

By
PAUL TORDA
I. P. VILLALBA
J. H. BRICK

POLYTECHNIC INSTITUTE OF BROOKLYN
BROOKLYN 2, NEW YORK
14 JUNE 1948

ACKNOWLEDGMENTS

The authors express their thanks to Dr. H. J. Heissner for his suggestions and advice, and to Professor D. E. Whitford for his careful checking of the final analysis.

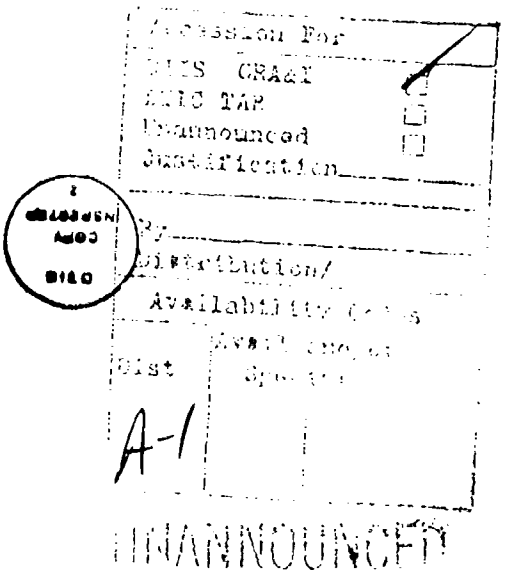

TABLE OF CONTENTS

COMPRESSIBLE FLOW THROUGH REED VALVES FOR PULSE JET ENGINES

I. HINGED REED VALVES

Paul Torda
I. P. Villalba
J. H. Brick

INTRODUCTION

A survey of the literature on pulse jet engines has shown some of the disadvantages of the reed type intake valves, such as restricted intake area, short reed endurance, etc. In meeting the problems indicated by research, investigators have increased the intake area by using conical, instead of flat reed valve banks. Some increase in reed life was also achieved by using neoprene coated and laminated reeds as well as neoprene coated valve seats.

In existing pulse jets the reeds move with undulating motion, i.e., they oscillate about their momentarily bent shapes. This means that for such reeds, as compared with reeds which form *smooth* nozzles throughout their motion, the inflow is restricted. Calculations carried out, but not presented here, have shown that for certain valve geometry and mass distribution this undulating motion of the reeds occurs. A basic postulate in the present analysis is that the reeds always form smooth nozzles throughout their motion. By this action of the reeds the inflow efficiency as well as the reed endurance increases. The prevention of oscillations about momentarily bent shapes of the reeds reduces their bending stresses. The bending stresses will be further reduced if the reeds are hinged instead of being clamped, as is customary, since the support constraints are reduced.

Numerous calculations have been carried out in order to determine the simplest method useful for numerical work. It is thought that the presented *closed form* solution of the non-linear differential equations fulfills this requirement.

The numerical examples are included as illustrations only. Although these numerical examples are believed to be correct, they do not include sufficient variation of the parameters involved to represent more than an illustration of the trend rather than complete data for purpose of design. The basic dimensions for the numerical examples were chosen to approximate those of the McDonnell 8-inch pulse jet engine.

This analysis shows that when *slender* valves and tapered mass distribution are combined non-undulating motion of the reeds occurs. Thus smooth inflow results and adverse transverse accelerations of the reeds are avoided.

The present report deals with the analysis of air inflow between hinged reeds. The case air inflow between clamped reeds is treated in a separate report.

AIR INFLOW ANALYSIS

In the present analysis the flow upstream of the valves was assumed parallel to the valve axis. This is equivalent to having a relatively short cowl ahead of a valve bank, the cowl diameter being large compared with the width of the individual valves, i.e., the valve bank being composed of a large number of valves. Isentropic change of state of the inflowing air was assumed, and a quasi-one-dimensional approach chosen. This latter approach takes into account the time variation of the flow area between the valves as well as the space and time variations of the flow velocity and pressure. , Figure 1, page 28.

The interaction between the inflow conditions, the valves, and the combustion chamber pressure is taken into account by satisfying the Euler dynamic equations, the continuity equation, the equation of change of state, and the equation of forced reed vibration. No theoretical or experimental data were available regarding the variation of the combustion chamber pressure behind the reeds. Therefore this pressure variation was calculated as a result of the analysis. The application of the results for design purposes is discussed briefly in section B, page 7.

The transition between inflow and combustion chamber conditions is taken into account by prescribing a physically probable velocity variation at an arbitrary time and an arbitrary cross section of the reed nozzle. This velocity variation can be modified easily to fit actual transition conditions as they are brought into evidence by better understanding of the aerothermodynamic process in the combustion chamber. Such a change would modify the numerical results but would not affect the analysis.

The requirement that the reeds form smooth nozzles throughout their motion influenced the choice of the space function, $X(x)$, of the analysis. The starting time, $t=0$, was chosen at a time when the reeds already are open slightly. This allowed the use of an exponential function for $X(x)$. If the starting time is to be chosen when the valves are closed, an additive function has to be used together with the exponential function. The additive function would complicate the expressions used for numerical work. Since the flow is well behaved during the very short time, Δt, which elapses while the valves open slightly, and its analysis would not yield significant results, the additive function could be left out of the analysis and the starting time defined as explained above. However, Δt, as well as the amount of slight opening, can be decreased arbitrarily without adverse effects on the results. The use of a single term for $X(x)$ greatly simplifies the numerical calculations.

This analysis considers non-steady, compressible flow between hinged reed valves during the period of opening. Once fully open, the valves will remain in this position until the pressure on the valve surface on the combustion chamber side exceeds that on the inflow side, at which time the valves will start to close. The numerical work could not be extended to include the closing period of the valves for lack of experimental as well as of analytical data on the pressure variation directly behind the valves.

For the convenience of the reader a list of symbols is presented ahead of the Appendix on page 16. The number designations of the equations are identical in the body of the report and in the Appendix. Thus equations missing in the report indicate intermediate steps which are given in the appendix.

(A) BASIC EQUATIONS DEFINING THE FLOW

The equation of continuity is:

$$\frac{\partial(\rho A)}{\partial t} + \frac{\partial(u\rho A)}{\partial x} = 0 \qquad \text{(a.1)}$$

The Euler dynamic equation of motion is:

$$\frac{\partial u}{\partial t} + u\frac{\partial u}{\partial x} + \frac{1}{\rho}\frac{\partial p}{\partial x} = 0 \qquad \text{(a.3)}$$

The equation of isentropic change of state is:

$$\frac{p}{p_0} = \left(\frac{\rho}{\rho_0}\right)^{\gamma} \qquad \text{(a.5)}$$

A new variable, $B = B(x,t)$, is defined as the product of the density, $\rho = \rho(x,t)$, and the cross sectional area between a pair of reeds, $A = A(x,t)$, or formally

$$B = B(x,t) = \rho(x,t)\, A(x,t) \qquad \text{(a.9)}$$

The continuity equation (a.1) then can be integrated to yield

$$u = \frac{1}{B}\left[K_1(t) - \int \frac{\partial B}{\partial t}\, dx\right] \qquad \text{(b.1)}$$

where $K_1(t)$, an arbitrary time function, arises in the integration.

Using the equation of isentropic change of state (a.5) and the expression for the velocity, u, (b.1) and its derivatives, the equation of motion (a.3) can be written in the form

$$\frac{\partial K_1(t)}{\partial t} - \int \frac{\partial^2 B}{\partial t^2} dx = -C_1 B\rho^{\gamma-2} \frac{\partial \rho}{\partial x} + \frac{2}{B} \frac{\partial B}{\partial t} \left[K_1(t) - \int \frac{\partial B}{\partial t} dx \right] + \qquad (b.3)$$

$$+ \frac{1}{B^2} \frac{\partial B}{\partial x} \left[K_1(t) - \int \frac{\partial B}{\partial t} dx \right]^2$$

Differentiation of eq. (b.3) with respect to x gives rise to a quadratic equation, the roots of which can be expressed as

$$\left[K_1(t) - \int \frac{\partial B}{\partial t} dx \right] = \frac{-D_2 \pm \sqrt{D_2^2 - 4D_1 D_3}}{2D_1} \qquad (b.6)$$

where D_1, D_2 and D_3 are functions of B and ρ, and are defined in Appendix - I, eq. (b.5).

The non-linear integro-differential equation, as given by (b.6), can be integrated in closed form if it is postulated that

(1) in the expression under the square root sign (a function of x and t) the variables are separable; and

(2) that in the expression (a.9) the variables are also separable. The use of the method of separation of variables restricts the domain of solutions. It is known, however, that the solutions thus obtained are sufficiently general.

Part (1) of the postulate reduces eq. (b.6) to two simultaneous equations and together with part (2) separates the variables in both of them. Thus we have the following:

From (1):

$$\left[K_1(t) - \int \frac{\partial B}{\partial t} dx \right] = \frac{-D_2 \pm \sqrt{\xi(x)\tau(t)}}{2D_1} \qquad (b.7a)$$

and

$$D_2^2 - 4D_1 D_3 = \xi(x)\tau(t) \qquad (b.7b)$$

and from (2):

$$B(x,t) = X(x)T(t) \qquad (b.9)$$

Differentiating eq. (b.7a) with respect to x and separating the variables in eqs. (b.7a and b.7b), the following equations are obtained

$$T = \beta e^{\lambda \int \sqrt{\tau}\, dt} \qquad (b.14)$$

and

and

$$\lambda = \frac{\frac{d\sqrt{\xi}}{dx}\left[2X\left(\frac{dX}{dx}\right)^2 - X^2\frac{d^2X}{dx^2}\right] + \sqrt{\xi}\left[6\left(\frac{dX}{dx}\right)^3 - 6\frac{dX}{dx}\frac{d^2X}{dx^2} + X^2\frac{d^3X}{dx^3}\right]}{X\frac{dX}{dx}\frac{d^3X}{dx^3} + \left(\frac{dX}{dx}\right)^2\frac{d^2X}{dx^2} - 2X\left(\frac{d^2X}{dx^2}\right)^2} \quad \text{(b.15)}$$

Equation (b.15) is a non-linear total differential equation in two undetermined functions of x, namely $X(x)$ and $\xi(x)$. Since the combination of the two functions must satisfy eq. (b.15), it is valid to choose one of the functions and determine the other from the differential equation.

Two different functions were chosen for $X(x)$ and the corresponding expressions for $\xi(x)$ were determined.

For case I

$$X_I(x) = be^{cx} \quad \text{(c.1)}$$

$$\xi_I(x) = \alpha_I e^{-2cx} \quad \text{(c.4)}$$

and for case II

$$X_{II}(x) = \{a_2(1-a_1)(x-a_3)\}^{\frac{1}{1-a_1}} \quad \text{(c.2)}$$

$$\xi_{II}(x) = \alpha_{II}^2\{a_2(1-a_1)(x-a_3)\}^{\frac{4a_1-6}{1-a_1}} \quad \text{(c.16)}$$

In the following the analysis is carried through for the exponential case (I) (eq. c.1) but for case (II) (eq. c.2) only the final results are given, since the procedure is identical in both cases.

Introducing the expressions for $X(x)$ and $\xi(x)$, as given by (c.1) and (c.4), into equation (b.7b) and integrating, the following expression is obtained for the density ($\rho=\rho(x,t)$).

$$\frac{1}{\gamma-1}\rho_I^{\gamma-1} = \frac{1}{C_1 c}\left\{\frac{\frac{d^2T_I}{dt^2}}{T_I} - \left(\frac{\frac{dT_I}{dt}}{T_I}\right)^2\right\}x - \frac{\tau_I\alpha_I}{8C_1c^2}e^{-2cx} - \frac{K_2(t)}{c}e^{-cx} + K_3(t) \quad \text{(c.7)}$$

where $K_2(t)$ and $K_3(t)$ are arbitrary time functions, arising in the integrations.

Introducing the expressions for $u(x,t)$, $B(x,t)$ and $\dot{X}(x)$, as given by equations (c.9,

b.9 and c.1 respectively), the Euler equation (a.3), after integration, yields a second expression for the density $\rho = \rho(x,t)$

$$\frac{1}{\gamma-1}\rho_I^{\gamma-1} = \frac{1}{C_1 c}\left\{\frac{\frac{d^2T_I}{dt^2}}{T_I} - \left(\frac{\frac{dT_I}{dt}}{T_I}\right)^2\right\} x - \frac{K_1(t)^2}{2T_I^2 b^2 C_1}e^{-2cx} + \frac{\frac{dK_1(t)}{dt}}{T_I b C_1 c}e^{-cx} + \frac{K_4(t)}{C_1} \qquad (c.10)$$

Expressions (c.7) and (c.10) must be identical for all values of the independent variables (x and t). Comparison of powers of x yields relationships between the time functions (see Appendix). The general expressions for the density, area and velocity distribution during inflow are

(c.13)

$$\rho_I = \left\{\frac{\gamma-1}{C_1}\left[\frac{d\tau_I}{dt}\frac{1}{c\sqrt{\tau_I}}\left(\frac{\sqrt{\alpha_I}}{4c^2}e^{-cx} - \frac{x}{2\lambda_I^2}\right) - \frac{\tau_I}{2c^3}\left(\frac{\alpha_I}{4c}e^{-2cx} + \frac{\sqrt{\alpha_I}}{\lambda_I^2}e^{-cx}\right) + K_4(t)\right]\right\}^{\frac{1}{\gamma-1}}$$

$$A_I = \frac{B}{\rho} = \frac{X(x)T(t)}{\rho} = b\rho_I\rho^{-1}e^{cx-\frac{1}{\lambda_I^2}\int\sqrt{\tau_I}\,dt} \qquad (c.14)$$

where ρ_I is given by equation (c.13), and

$$u_I = \frac{\sqrt{\tau_I}}{c}\left\{\frac{\sqrt{\alpha_I}}{2c}e^{-cx} + \frac{1}{\lambda_I^2}\right\} \qquad (c.15)$$

Using the function for X(x), as given in case II

$$X_{II}(x) = \{a_2(1-a_1)(x-a_3)\}^{\frac{1}{1-a_1}} \qquad (c.2)$$

the general expressions for the density, area and velocity are found to be

$$\rho_{II} = \left\{\frac{\gamma-1}{C_1}\left[(x-a_3)^2\left(\frac{\lambda_{II}}{2\sqrt{\tau_{II}}}\frac{d\tau_{II}}{dt} - 2\lambda_{II}^2\tau_{II}\right) + \frac{2}{3}\left(-\frac{a_2}{2}\right)^{\frac{3}{2}}\frac{\alpha_{II}}{a_2^3}(x-a_3)^{\frac{3}{2}}\left(\frac{1}{\sqrt{\tau_{II}}}\frac{d\tau_{II}}{dt} - 6\lambda_{II}^2\tau_{II}\right) + \frac{\alpha_{II}^2}{4a_2^3}\tau_{II}^2 x - K_5(t)\right]\right\}^{\frac{1}{\gamma-1}} \qquad (c.18)$$

$$A_{II} = \frac{B}{\rho} = \frac{X(x)T(t)}{\rho} = \beta_{II} e^{\lambda_{II}\int\sqrt{\tau_{II}}dt} \{-2a_2(x-a_3)\}^{-\frac{1}{2}} \rho_{II}^{-1} \qquad (c.19)$$

Where ρ_{II} is given by eq. (c.18), and

$$u_{II} = \sqrt{\tau_{II}} \left\{ \frac{\alpha_{II}}{2a_2^2} \left[-2a_2(x-a_3) \right]^{\frac{1}{2}} - 2\lambda_{II}(x-a_3) \right\} \qquad (c.20)$$

The results, obtained so far, have to be adapted to the particular problem at hand.

(B) SOLUTION OF THE BOUNDARY VALUE PROBLEM

The expressions for density, velocity, and area distribution of the flow, as given above for cases I and II, represent solutions of the basic equations (a.1), (a.3), and (a.5). The arbitrary constants and time functions in these expressions must be determined for the boundary value problem under consideration. The undetermined time function, $\tau(t)$, which appears in these expressions, determines the pressure, velocity, and area variations throughout the air inflow.

This time function, $\tau(t)$, should be derived from the transition condition between the air inflow and the aero-thermodynamic process in the combustion chamber. It was not possible to do this, since, as was stated in the introduction, insufficient data were available. It was necessary, therefore, to select a function, the use of which would result in a physically probable solution of the problem.

The function $\tau(t)$ was selected by prescribing a time variation of the inflow velocity at some arbitrary position along the X axis. Two functions were used for $\tau(t)$ bounding the entire domain of possible variations. For design purposes numerical analyses should be carried out for many other examples within this domain, similar to those presented. The designer can then select the proper valve parameters by comparison of the results of these numerical examples with the particular combustion chamber pressure variation of interest to him.

For the inflow between hinged reed valves, the initial and boundary conditions to be satisfied may be stated as follows:

1. At the inlet section (x=0) the area of inflow must be constant for any time (t). This can be expressed

   for $x = 0$

$$A(0,t) = \text{constant} = A_{o,t} = A_{o,o} \qquad \text{(d.1a)}$$

2. At the start of the inflow (t=0) the density at the inlet section is very close to stagnation density, so that with sufficient numerical accuracy $\rho(0,0)=\rho_s$. From equation (a.9), therefore

for $x = 0$ and $t = 0$

$$B(0,0) = \rho_s A_{o,o} \qquad \text{(d.1b)}$$

3. For the start of the inflow (t=0) and the exit section (x=h) there is for zero area a singularity point in the B function, as has been explained earlier in the beginning of *AIR INFLOW ANALYSIS*, page 2. This point has been excluded from the analysis. It should be pointed out, however, that the area at this point and time may be made arbitrarily small without detriment to the condition on the density. The density at this point and time is slightly less than the density at the inlet section, so that a nearly constant density distribution along x results for t=0. The amount of gap between the valves at the exit section can be so chosen as to give this desired density distribution. This condition can be expressed

for $t = 0$ and $x = h$

$$B(h,o) \simeq \rho_s A_{h,o} \qquad \text{(d.1c)}$$

4. At the end of the opening time ($t=t_1$), the density at the exit section [$\rho(h,t_1)$], and the area at the exit section [$A(h,t_1)$] should be prescribed values. This condition can be expressed as

$$B(h,t_1) = \mu\rho_s \nu A_{o,o} \qquad \text{(d.1d)}$$

where the constants μ, ν have to be

$$\mu < 1$$
$$\nu \leq 1$$

The choice of ν, however, is governed by the fact that the reeds in the fully open position must present a somewhat inclined surface facing the combustion chamber, so that the 'closing' pressure can build up behind the reeds.

5. As has been pointed out previously an appropriate time variation of the velocity, at some defined position, e.g. at the entrance (x=0), had to be prescribed. The opening of the reeds was considered to occur during the maximum pressure difference on both sides of the valve reeds. Thus, it seemed to be appropriate to prescribe this ve-

locity variation to increase from a small initial value towards that of a maximum during the inflow. This can be expressed

for $x = 0$ as

$$u(o,t) = f(t) \tag{d.1e}$$

Again the analysis is given for case I only (i.e. where $X(x) = be^{cx}$) and the resulting expressions for case II

(i.e. where $X(x) = \{a_2(1-a_1)(x-a_1)\}^{\frac{1}{1-a_1}}$)

are included at the end of this section.

The arbitrary function of time $K_4(t)$ in equation (c.14) was determined from the condition that the area at the inlet section be constant for any time (d.1a). Substituting the values $x=0$ and $A=A_{o,o}$ in equation (c.14), $K_4(t)$ was found to be

$$K_4(t) = \frac{C_1}{\gamma-1}\left\{\frac{A_{o,o}}{b\beta_I}\, e^{\frac{1}{\lambda_I^2}\int\sqrt{\tau_I}\,dt}\right\}\left\{-\frac{\sqrt{\alpha_I}}{4c^3}\frac{d\tau_I}{dt}\frac{1}{\sqrt{\tau_I}} + \frac{\tau_I}{2c^3}\left\{\frac{\alpha_I}{4c} + \frac{\sqrt{\alpha_I}}{\lambda_I^2}\right\}\right. \tag{d.3}$$

The arbitrary constants b and β_I appear in equation (c.14) only as a product term, and this product could, therefore, be evaluated from condition (d.1b), i.e.

$$B(o,o) = \rho_s A_{o,o} \tag{d.4}$$

Recalling that $B=B(x,t)$ has been defined to be $B=\rho.A$ equation (a.9) and using equations (c.13 and c.14), the constant c has been determined from condition (d.1c). Here the fact that the density at $x=h$ and $t=o$ is only approximately equal to that of the stagnation density, has been neglected, since in the numerical evaluations it has been found that $\rho(h,o) = .996\rho_s$. Thus $\rho(h,o) = \rho_s$ was used. Thus

$$c = \frac{1}{h}\, ln\, \frac{A_{h,o}}{A_{o,o}} \tag{d.5}$$

For the determination of the unknown time function, $\tau(t)$, the velocity distribution at the entrance to the valves, condition (d.1e), has been selected as

$$u(o,t) = b_o + b_1 t + \ldots + b_n t^n = \sum_{n=o}^{n} b_n t^n \equiv f(t) \tag{d.6}$$

and $\tau(t)$ expressed from (d.6) and (c.15)

$$\tau_I(t) = \frac{c^2 f(t)^2}{\left\{ \frac{\sqrt{\alpha_I}}{2c} + \frac{1}{\lambda_I^2} \right\}} \tag{d.7}$$

Using condition (d.1d) and equations (c.13 and c.14) $\sqrt{\alpha_I}$ is calculated

$$\sqrt{\alpha_I} = \frac{2c}{\lambda_I^2} (\Delta_I - 1) \tag{d.11}$$

where

$$\Delta_I = \frac{c[\int f(t)dt]_{t_1}}{ch - ln\ \mu\nu} \tag{d.10}$$

Inserting the values of the constants and arbitrary functions of time, as were determined from the boundary conditions, into equations (c.13, c.14 and c.15), and noting that λ_I is eliminated from the expressions by this process, the final expressions used for the numerical examples are as follows:

$$\rho_I = \left\{ \frac{\gamma-1}{C_1} \left[\frac{f_2(t)}{\Delta_I} \left(\frac{\Delta_I - 1}{c} (e^{-cx} - 1) - x \right) - \frac{f(t)^2}{\Delta_I^2} \left(\frac{(\Delta_I - 1)^2}{2} (e^{-2cx} - 1) + \right. \right. \right.$$

$$\left. \left. \left. + (\Delta_I - 1)(e^{-cx} - 1) \right) + \frac{C_1}{\gamma - 1} \rho_s^{\gamma-1} e^{\frac{1-\gamma}{\Delta_I} c f_1(t)} \right] \right\}^{\frac{1}{\gamma-1}} \tag{d.12}$$

$$A_I = A_{o,o} \rho_s e^{cx - \frac{c f_1(t)}{\Delta_I}} \left\{ \rho_I \right\}^{-1} \tag{d.13}$$

where ρ_I is given by (d.12)

$$u_I = \frac{f(t)}{\Delta_I} \{ (\Delta_I - 1)\, e^{-cx} + 1 \} \tag{d.14}$$

The expressions for Case II are

(d.24)

$$\rho_{II} = \left\{ \frac{\gamma-1}{C_1} \left[\left(\frac{F_2(t)}{\Delta_{II} + 2a_3} - 2 \frac{F(t)^2}{[\Delta_{II} + 2a_3]^2} \right) \left((x - a_3)^2 - a_3^2 \right) - \right. \right.$$

$$-\frac{1}{3}\left(-\frac{1}{a_3}\right)^{\frac{1}{2}}\Delta_{II}\left(2\frac{F_2(t)}{\Delta_{II}+2a_3}-6\frac{F(t)^2}{[\Delta_{II}+2a_3]^2}\right)\left((x-a_3)^{\frac{3}{2}}-(-a_3)^{\frac{3}{2}}\right)+$$

$$+\frac{\Delta_{II}^2F(t)^2x}{2a_3[\Delta_{II}+2a_3]^2}+\frac{C_1}{\gamma-1}\rho_s^{\gamma-1}\left.e^{-(1-\gamma)\frac{F_1(t)}{\Delta_{II}+2a_3}}\right]\Bigg\}^{\frac{1}{\gamma-1}}$$

$$A_{II}=A_{o,o}\rho_s\left\{-\frac{a_3}{x-a_3}\right\}^{\frac{1}{2}}e^{\frac{F_1(t)}{\Delta_{II}+2a_3}}\left\{\rho_{II}\right\}^{-1} \qquad (d.25)$$

where ρ_{II} is given by (d.24)

$$u_{II}=F(t)\left\{\frac{\Delta_{II}\left[-\frac{x-a_3}{a_3}\right]^{\frac{1}{2}}-2(x-a_3)}{\Delta_{II}+2a_3}\right\} \qquad (d.26)$$

Thus far the flow equations were discussed and solved for the present boundary value problem. To adapt the reed shapes to the bounding stream-line pattern, it is necessary to investigate the forces acting upon them. This was done by considering the differential equation of reed motion.

(C) DETERMINATION OF THE MASS DISTRIBUTION AND INERTIA PROPERTIES OF THE REEDS

The mass distribution of the reeds was determined from the equation expressing the equilibrium between the pressure forces acting on both sides of the reeds and their elastic and inertia forces.

The differential equation for the forced vibration of a reed is

$$\frac{\partial^2\left(EI\frac{\partial^2y}{\partial x^2}\right)}{\partial x^2}+m\frac{\partial^2y}{\partial t^2}=q(x,t) \qquad (e.1)$$

Considering the equilibrium of forces over a small element of the reed, for which the moment of inertia was considered constant, this equation reduces to

$$EI \frac{\partial^4 y}{\partial x^4} + m \frac{\partial^2 y}{\partial t^2} = q(x,t) \qquad \text{(e.1a)}$$

The forcing function $q(x,t)$ consists of known pressure forces on the inflow side, and of unknown pressure forces on the combustion chamber side of the reeds. As was stated earlier in the report, no theoretical or experimental evidence was available to indicate the form of the pressure variation downstream of the valves, and, therefore, for a prescribed mass distribution of the reed the pressure variation on the combustion chamber side of reeds was calculated from the following equation.

$$q_{cc}(x,t) = q_i(x,t) - EI\frac{\partial^4 y}{\partial x^4} - m\frac{\partial^2 y}{\partial t^2} \qquad \text{(e.1b)}$$

For the specific mass distributions chosen in the numerical calculations, the variations of pressure on the combustion chamber side of the reeds obtained from equation (e.1b) appeared to be qualitatively correct.

The numerical examples, included as illustrations of the analysis, can now be presented.

(D) ILLUSTRATIVE EXAMPLES

The numerical calculations presented in this paper were guided by considerations of actual pulse-jet engines now in existence. Inasmuch as very little reliable experimental data related to the air inflow problem exists, the numerical values of the parameters were chosen with a view towards establishing general trends.

The basic valve dimensions were chosen as closely as possible to those of the 8 inch McDonnell pulse-jet engine.

Preliminary calculations indicated that, for a given valve length, the ratio of inlet area to exit area at the beginning of the cycle should be relatively small to prevent excessive transverse acceleration of the reeds at the exit section.

A suitably chosen mass distribution of the reeds then enables them to follow the instantaneous bounding streamlines.

In the numerical work it was assumed that the pulse-jet was operating at sea level con-

ditions with a forward velocity of 500 m.p.h. This velocity was thought to be compatible with the present applications of the pulse jets. The inflow time as a percentage of the total cycle time was unknown and was, therefore, chosen from analysis of pressure graphs as approximately 1/3 of the period, and the opening time of the valves to be 1/6 of the total period.

The significance of the area ratio $\left(\frac{A_{o,o}}{A_{h,o}}\right)$ led to the choice of this parameter as a basic one and, for a valve length of one inch, the following values were used for the numerical calculations:

Case I $\quad \frac{A_{o,o}}{A_{h,o}} = \quad 3:1 \quad \& \quad 5:1$

Case II $\quad \frac{A_{o,o}}{A_{h,o}} = \quad 3.33:1$

Following the method described in chapter (c) the values of the arbitrary constants and the arbitrary time functions were determined from the boundary conditions formulated there.

The types of velocity distributions at the entrance of the valves were chosen as shown in Fig. 2. This figure shows that, for the smaller area ratios (3:1 and 3.33:1), higher intake velocities result. The three velocity curves with increasing tangents (Nos. 1, 2, 4) result in slower opening of the reeds at the beginning of the movement, whereas in the case of the curve with decreasing tangents (No. 3) the rate of opening is greater at the start. Thus, higher reed accelerations result for curves 1, 2 and 4 at the end of the reed movement than for curve 3. This latter curve (3) also permits greater filling of the combustion chamber during the opening of the valves, as can be seen by a comparison of the areas under the curves.

Figures 3 to 6 incl. represent the air intake velocity distribution (u) as a function of the inflow direction (x) for various times (t). A comparison of Figs. 3, 5 and 6 shows that, for case I (the exponential case), and an area ratio approximately 3:1 (Figs. 3 and 5), the velocity distribution with time is much more regular than for case II (the polynomial case) (Fig. 6). This is probably due to the difference in the original curvature of the reeds. For convenience dimensionless coordinates $\left(u_D = \frac{u}{u_o} \text{ and } x_D = \frac{x}{h}\right)$ are included in the graphs.

Fig. 7 shows the scale drawings of the reeds in their initial and final positions for both cases and all area ratios.

Figs. 8-11 incl. show the instantaneous streamline shapes for various times (t). A comparison of these figures shows.

(1) that the exponential case (I) gives smoother streamlines than the polynomial case (II),

(2) that the reed movement in the case of the velocity curve with decreasing tangents (curve 3 Fig. 2) yields less acceleration than the other velocity curves, and

(3) that the reeds for case I and area ratio 5:1 would have to suffer great bending deflections if they were to follow the instantaneous streamlines. This would be possible only if the reeds were extremely thin and, therefore, impractical from the design standpoint.

Figs. 12-15 incl. show the variation of the inflow pressure versus distance along the direction of flow (x) for various times (t). Again a more advantageous pressure variation with time is obtained with the velocity distribution of curve (3) Fig. 2.

The values for $\frac{\partial^2 y}{\partial t^2}$ and $\frac{\partial^4 y}{\partial x^4}$, needed for the evaluation of eq. (e.1b), giving the pressure distribution on the combustion chamber side of the reeds, are plotted in Figs. 16-19 incl. for case I and for area ratios 3:1 and 5:1 only. Figs. 17 and 19 show that the accelerations and bending of the reeds for the 5:1 area ratio are excessive.

Figs. 20 and 21 show how the variation of the pressures on both sides of the reeds in non-dimensional form. The curves show that the combustion chamber pressures are functions of time and space.

CONCLUSIONS

The analysis shows that for efficient filling of the combustion chamber of pulse-jet engines a large number of tightly spaced reed valves should be employed.

The necessity of handling large amounts of air is still doubted by some investigators. Present day trend of pulse jet design, however, seems to confirm the opinion expressed in the introduction, namely, that for an efficient aero-thermodynamic process of the pulse-jet the 'restriction' of the intake valves should be reduced.

No attempt was made in this paper to suggest spatial reduction of the intake restriction. Work towards this effect has been going on for some time at PIBAL. Here the attempt was

made to investigate the possibility of aerodynamic and mechanical improvement of the reed valves.

Numerical work along the lines laid down here, should be continued in order to establish the effect of the variation of all possible parameters, thus presenting data for the designer on a broader basis and possibly in a graphical, and, therefore, more useful form.

LIST OF SYMBOLS

a_1 ; a_2 ; a_3 ;	constants in $X_{II}(x)$ function
$A(x,t)$	area variable, denoting cross sectional area between a pair of reeds
$A_{o,o}$	cross sectional area between a pair of reeds at x=0, t=0
$A_{o,t}$	cross sectional area between a pair of reeds at x=0, t=t
$A_{h,o}$	cross sectional area between a pair of reeds at x=h, t=0
$A_{h,t}$	cross sectional area between a pair of reeds at x=h, t=t
α	constant in $\xi(x)$ functions
b	constant in $X_I(x)$ function
$B(x,t) = \rho(x,t)\, A(x,t)$	product of density and area variables
β	constant in $T(t)$ function
c	constant in $X_I(x)$ function
$C_1 = \gamma \frac{p_o}{\rho_o{}^{\gamma}}$	constant
c_p	specific heat at constant pressure
c_v	specific heat at constant volume
$\gamma = \frac{c_p}{c_v} = 1.4$	adiabatic constant
$D_1, D_2, D_3,$	functions of $B(x,t)$ and $\rho(x,t)$, defined in eqs. (b.5)
Δ	constant
E (lb/in^2)	modulus of elasticity of reed material

$h(in)$	length of the reed
$I\ (in^4)$	moment of inertia of the reed cross section
$k\ (in)$	half distance between a pair of reeds
$K_1(t); K_2(t); K_3(t); K_4(t); K_5(t)$	arbitrary functions of time arising in integrations
λ	constant arising in separation of variables
$m\ (\frac{lb\ sec^2}{in^2})$	mass of the reed per unit length
μ	density factor
ν	area factor
$p(x,t)$	pressure variable
$q(x,t)$	forcing function, resultant pressure on both sides of the reed (lb/in)
$q_i(x,t)$	pressure on the intake side of the reed (lb/in)
$q_{cc}(x,t)$	pressure on the combustion chamber side of the reed (lb/in)
$\rho(x,t)$	density variable
ρ_s	stagnation density
t	time variable
t_1	opening time
$T(t)$	time function
$\tau(t)$	time function
$u(x,t)$	velocity variable

$V = \rho^{\gamma-2}\frac{\partial \rho}{\partial x}$	density function
w (in)	depth of reed valve
x	space variable
$X(x)$	space function
$\xi(x)$	space function
$y(x,t)$	dependent space variable

subscript zero refers to free stream conditions

subscript I and II denote two specific cases in the numerical examples.

APPENDIX

QUASI ONE-DIMENSIONAL INFLOW BETWEEN REED VALVES

(A) BASIC EQUATIONS DEFINING THE FLOW

The equation of continuity can be written:

$$\frac{\partial(\rho A)}{\partial t} + \frac{\partial(u\rho A)}{\partial x} = 0 \qquad \text{(a.1)}$$

where

$A = A(x,t)$	is the cross sectional area	(a.2)
$\rho = \rho(x,t)$	is the density of the gas	
$u = u(x,t)$	is the velocity of the flow	
x	is the coordinate in the direction of the flow	
t	is the time	

The Euler equation of flow is:

$$\frac{\partial u}{\partial t} + u\frac{\partial u}{\partial x} + \frac{1}{\rho}\frac{\partial p}{\partial x} = 0 \qquad \text{(a.3)}$$

where $p = p(x,t)$ is the pressure of the gas and u, ρ, x, t are defined in (a.2). (a.4)

Tlhe equation describing adiabatic change of state is:

$$\left(\frac{\rho}{\rho_o}\right)^{\gamma} = \frac{p}{p_o} \qquad \text{(a.5)}$$

where

p_o	is the free stream pressure	(a.6)
ρ_o	is the free stream density	
$\gamma = \frac{c_p}{c_v}$	is the adiabatic constant	
c_p and c_v	are specific heat at constant pressure and constant volume respectively.	

Using eq. (a.5), eq. (a.3) can be written:

$$\frac{\partial u}{\partial t} + u\frac{\partial u}{\partial x} + C_1 \rho^{\gamma-2}\frac{\partial \rho}{\partial x} = 0 \qquad (a.7)$$

where

$$C_1 = \frac{\gamma p_o}{\rho_o{}^{\gamma}} = \text{const.} \qquad (a.8)$$

Introducing a new variable (B), being the product of the area (A) and density (ρ), i.e.:

$$B = \rho . A = B(x,t) \qquad (a.9)$$

equation (a.1) can be written:

$$\frac{\partial B}{\partial t} + u\frac{\partial B}{\partial x} + B\frac{\partial u}{\partial x} = 0 \qquad (a.10)$$

(B) INTEGRATION OF THE BASIC EQUATIONS

Using the method of variation of parameters, the continuity equation in its rewritten form (a.10) can be integrated to yield an expression for the flow-velocity:

$$u = \frac{1}{B}\left[K_1(t) - \int \frac{\partial B}{\partial t}\,dx\right] \qquad (b.1)$$

where $K_1(t)$ is an arbitrary function of time arising from the integration.

Substuting u and its derivatives into eq. (a.7), we obtain:

$$C_1 \rho^{\gamma-2}\frac{\partial \rho}{\partial x} = \frac{1}{B^2}\left\{\frac{\partial B}{\partial t}\left[K_1 - \int \frac{\partial B}{\partial t}\,dx\right] - B\left[\frac{\partial K_1}{\partial t} - \int \frac{\partial^2 B}{\partial t^2}\,dx\right]\right\} + \frac{1}{B^3}\left\{\left[K_1 - \int \frac{\partial B}{\partial t}dx\right]\left(B\frac{\partial B}{\partial t} + \frac{\partial B}{\partial x}\left[K_1 - \int \frac{\partial B}{\partial t}\right]dx\right)\right\} \qquad (b.2)$$

or, after rearranging:

$$\left[\frac{\partial K_1}{\partial t} - \int \frac{\partial^2 B}{\partial t^2}\, dx\right] = -C_1 B\rho^{\gamma-2} \frac{\partial \rho}{\partial x} + \frac{2}{B}\frac{\partial B}{\partial t}\left[K_1 - \int \frac{\partial B}{\partial t}\, dx\right] + \tag{b.3}$$

$$+ \frac{1}{B^2}\frac{\partial B}{\partial x}\left[K_1 - \int \frac{\partial B}{\partial t}\, dx\right]^2$$

Differentiating eq. (b.3) with respect to x and arranging terms, we obtain:

$$D_1\left[K_1 - \int \frac{\partial B}{\partial t}\, dx\right]^2 + D_2\left[K_1 - \int \frac{\partial B}{\partial t}\, dx\right] + D_3 = 0 \tag{b.4}$$

where

$$\left.\begin{aligned} D_1 &= \frac{1}{B^3}\left[2\left(\frac{\partial B}{\partial x}\right)^2 - B\frac{\partial^2 B}{\partial x^2}\right] \\ D_2 &= \frac{1}{B^2}\left[4\frac{\partial B}{\partial x}\frac{\partial B}{\partial t} - 2B\frac{\partial^2 B}{\partial x \partial t}\right] \\ D_3 &= C_1\left\{B\rho^{\gamma-2}\frac{\partial \rho}{\partial x} + \frac{\partial}{\partial x}\left[B\rho^{\gamma-2}\frac{\partial \rho}{\partial x}\right]\right\} + \frac{2}{B}\left(\frac{\partial B}{\partial t}\right)^2 - \frac{\partial^2 B}{\partial t^2} \end{aligned}\right\} \tag{b.5}$$

Noting that eq. (b.4) is a quadratic, we can write:

$$\left[K_1 - \int \frac{\partial B}{\partial t}\, dx\right] = \frac{-D_2 \pm \sqrt{D_2^2 - 4D_1 D_3}}{2D_1} \tag{b.6}$$

Equating the discriminant to a (yet to be determined) function of x and t, in which however, the variables should be separated, we get two simultaneous equations instead of eq. (b.6):

$$\left[K_1 - \int \frac{\partial B}{\partial t}\, dx\right] = \frac{-D_2 \pm \sqrt{\xi \cdot \tau}}{2D_1} \tag{b.7a}$$

$$D_2^2 - 4D_1 D_3 = \xi \cdot \tau \tag{b.7b}$$

where $\xi = \xi(x)$ and $\tau = \tau(t)$ (b.8)

Assuming the solution of eq. (a.9), giving the expression for ρA, in the form:

$$B(x,t) = X(x).\ T(t) = XT \tag{b.9}$$

eq. (b.7a) reduces to:

$$\left[K_1 - \frac{dT}{dt}\int X dx\right] = -\frac{\frac{dX}{dx} X^2 \frac{dT}{dt}}{2\left(\frac{dX}{dx}\right)^2 - X\frac{d^2X}{dx^2}} \pm \frac{\sqrt{\xi}\sqrt{\tau}\, X^3 T}{4\left(\frac{dX}{dx}\right)^2 - 2X\frac{d^2X}{dx^2}} \tag{b.10}$$

and eq. (c.7b) can be transformed to:

$$\frac{\partial}{\partial x}\left[\rho^{\gamma-2}\frac{\partial \rho}{\partial x}\right] + \left[\rho^{\gamma-2}\frac{\partial \rho}{\partial x}\right]\left\{\frac{X\frac{dX}{dx}\frac{d^2X}{dx^2} - 2\left(\frac{dX}{dx}\right)^3}{X^2\frac{d^2X}{dx^2} - 2X\left(\frac{dX}{dx}\right)^2}\right\} =$$

$$= \frac{\xi\tau X^2}{4C_1\left[X\frac{d^2X}{dx^2} - 2\left(\frac{dX}{dx}\right)^2\right]} + \frac{\left(\frac{dT}{dt}\right)^2}{C_1 T^2}\left\{\frac{3\left(\frac{dX}{dx}\right)^2 - 2X\frac{d^2X}{dx^2}}{X\frac{d^2X}{dx^2} - 2\left(\frac{dX}{dx}\right)^2}\right\} + \frac{\frac{d^2T}{dt^2}}{C_1 T} \tag{b.11}$$

Differentiating eq. (b.10) with respect to X and separating variables, this equation can be written:

$$\pm \frac{2\frac{dT}{dt}}{T\sqrt{\tau}} = \frac{\frac{d\sqrt{\xi}}{dx}\left[2X\left(\frac{dX}{dx}\right)^2 - X^2\frac{d^2X}{dx^2}\right] + \sqrt{\xi}\left[6\left(\frac{dX}{dx}\right)^3 - 6X\frac{dX}{dx}\frac{d^2X}{dx^2} + X^2\frac{d^3X}{dx^3}\right]}{X\frac{dX}{dx}\frac{d^3X}{dx^3} + \left(\frac{dX}{dx}\right)^2\frac{d^2X}{dx^2} - 2X\left(\frac{d^2X}{dx^2}\right)^2} = \lambda \tag{b.12}$$

where λ is a constant.

Choosing the positive sign of the square root expression, from equation (b.12) we have:

$$\frac{1}{T}\frac{dT}{dt} = \lambda\sqrt{\tau} \tag{b.13}$$

and integrating, we get:

$$T = \beta e^{\lambda\int\sqrt{\tau}\,dt} \tag{b.14}$$

Equation (b.12) also yields:

$$\frac{\frac{d\sqrt{\xi}}{dx}\left[2X\left(\frac{dX}{dx}\right)^2 - X^2\frac{d^2X}{dx^2}\right] + \sqrt{\xi}\left[6\left(\frac{dX}{dx}\right)^3 - 3X\frac{dX}{dx}\frac{d^2X}{dx^2} + X^2\frac{d^3X}{dx^3}\right]}{X\frac{dX}{dx}\frac{d^2X}{dx^2} + \left(\frac{dX}{dx}\right)^2\frac{d^2X}{dx^2} - 2X\left(\frac{d^2X}{dx^2}\right)^2} = \lambda \tag{b.15}$$

(C) SPECIAL SOLUTIONS

Two examples are worked out in this report.

Case I. $X_I = X_I(x) = be^{cx}$ (c.1)

Case II $X_{II} = X_{II}(x) = \left\{a_2(1-a_1)(x-a_3)\right\}^{\frac{1}{1-a_1}}$ (c.2)

Case C.I. Using equation (c.1) in equation (b.15) above, the denominator, transposed to the right side, becomes zero. Equating the numerator (or left hand side) to zero and simplifying, one obtains;

$$\frac{1}{\sqrt{\xi_I}}\frac{d\sqrt{\xi_I}}{dx} + c = 0 \tag{c.3}$$

Integrating (c.3), we obtain an expression for ξ_I, to be:

$$\sqrt{\xi_I} = \alpha_I^{\frac{1}{2}} e^{-cx}$$

and therefore:

$$\xi_I = \alpha_I e^{-\frac{1}{2}cx} \tag{c.4}$$

Introducing into equation (b.11) the values of X_I, given by expression (c.1), and ξ_I, given by expression (c.4), and still using the symbol T_I, instead of expression (b.14) for brevity, equation (b.11) yields:

$$T_I = \beta_I e^{\lambda_I \int \sqrt{\tau_I}\, dt} \tag{b.14a}$$

$$\frac{\partial V}{\partial x} + cV = \left\{ \frac{1}{C_1 T_I} \frac{d^2 T_I}{dt^2} - \frac{1}{C_1 T_I^2} \left(\frac{dT_I}{dt} \right)^2 \right\} - \frac{\tau_I}{4 C_1 c^2} \alpha_I e^{-\frac{1}{2}cx} \tag{c.5}$$

where

$$V = \rho^{\frac{\gamma-1}{2}} \frac{\partial \rho}{\partial x} \tag{c.6}$$

Using the method of variation of parameters, equation (c.5), when integrated twice with respect to x, yields:

$$\frac{1}{\gamma-1} \rho_I^{\gamma-1} = \frac{1}{C_1 c} \left\{ \frac{1}{T_I} \frac{d^2 T_I}{dt^2} - \frac{1}{T_I^2} \left(\frac{dT_I}{dt} \right)^2 \right\} x - \frac{\tau_I \alpha_I}{8 C_1 c^4} e^{-\frac{1}{2}cx} - \tag{c.7}$$

$$- \frac{1}{c} K_2(t) e^{-cx} + K_3(t)$$

where $K_2(t)$ and $K_3(t)$ are arbitrary functions of time arising from the integrations. Using the value for X_I from equation (c.1) and recalling that B was given as:

$$B(x,t) = \rho . A = X . T \tag{b.9}$$

B can now be expressed:

$$B_I = b T_I e^{cx} \tag{c.8}$$

and thus the expression (b.1) for u becomes

$$u_I = \frac{1}{bT_I} K_1 e^{-cx} - \frac{1}{cT_I} \frac{dT_I}{dt} \qquad (c.9)$$

Inserting this value of u, and its derivatives into the Euler dynamic equation (a.3), and integrating, we get a second expression for ρ_I.

$$\frac{1}{\gamma-1} \rho_I^{\gamma-1} = \frac{1}{C_1 c} \left\{ \frac{1}{T_I} \frac{d^2T_I}{dt^2} - \frac{1}{T_I^2} \left(\frac{dT_I}{dt} \right)^2 \right\} x - \qquad (c.10)$$

$$- \frac{1}{2T_I^2 b^2 C_1} K_1^2 e^{-2cx} + \frac{1}{T_I b C_1 c} \frac{dK_1}{dt} e^{-cx} + \frac{K_4}{C_1}$$

Comparing coefficients of equal powers of x in equations (c.7) and (c.10), we obtain the following relations between the arbitrary time functions which arose from the integrations:

$$K_1(t) = K_1 = \frac{b}{2c^2} T_I \sqrt{\alpha_I \tau_I}$$

$$K_2(t) = K_2 = \frac{\sqrt{\alpha_I}}{2C_1 c^2} \left\{ - \frac{1}{2\sqrt{\tau_I}} \frac{d\tau_I}{dt} - \frac{\sqrt{\tau_I}}{T_I} \frac{dT_I}{dt} \right\} \qquad (c.11)$$

$$K_3(t) = K_3 = \frac{K_4(t)}{C_1}$$

or by substituting expression (b.14) for T, and letting $\lambda = \lambda_I$

$$K_1(t) = \frac{b\beta_I}{2c^2} \sqrt{\alpha_I \tau_I} \, e^{-\frac{1}{\lambda_I^2} \int \sqrt{\tau_I} \, dt}$$

$$K_2(t) = \frac{\sqrt{\alpha_I}}{2C_1 c^2} \left\{ \frac{\tau_I}{\lambda_I^2} - \frac{1}{2\sqrt{\tau_I}} \frac{d\tau_I}{dt} \right\} \qquad (c.11a)$$

$$K_3(t) = \frac{K_4(t)}{C_1}$$

Thus the following expressions are obtained:

$$B_I = \rho_I A_I = b\beta_I e^{cx - \frac{1}{\lambda_I^2}\int\sqrt{\tau_I}\,dt} \qquad (c.12)$$

(c.13)

$$\rho_I = \left\{ \frac{\gamma-1}{C_1}\left[\frac{1}{c\sqrt{\tau_I}} \frac{d\tau_I}{dt}\left(\frac{\sqrt{\alpha_I}}{4c^2} e^{-cx} - \frac{x}{2\lambda_I^2} \right) - \frac{\tau_I}{2c^3}\left(\frac{\alpha_I}{4c} e^{-2cx} + \frac{\sqrt{\alpha_I}}{\lambda_I^2} e^{-cx} \right) + K_4 \right] \right\}^{\frac{1}{\gamma-1}}$$

$$A_I = b\beta_I e^{cx - \frac{1}{\lambda_I^2}\int\sqrt{\tau_I}\,dt} \left\{ \rho_I^{-1} \right\} \qquad (c.14)$$

$$u_I = \frac{\sqrt{\tau_I}}{c}\left\{ \frac{\sqrt{\alpha_I}}{2c} e^{-cx} + \frac{1}{\lambda_I^2} \right\} \qquad (c.15)$$

Case C.II. Using the expression (c.2) for X_{II}:

$$X_{II} = X_{II}(x) = \{a_2(1-a_1)(x-a_3)\}^{\frac{1}{1-a_1}} \qquad (c.2)$$

Substituting (c.2) in equation (b.15) and integrating:

$$\xi_{II} = \alpha_{II}^2 \{a_2(1-a_1)(x-a_3)\}^{\frac{4a_1-3}{1-a_1}} \qquad (c.16)$$

and T_{II} is defined by equation (b.14)

$$T_{II} = \beta_{II} e^{\lambda_{II} \int \sqrt{\tau_{II}}\, dt} \tag{b.14b}$$

Employing the same method as for case C.I., the following expressions are obtained for $B_{II}(x,t)$, $\rho_{II}(x,t)$, $A_{II}(x,t)$ and $u_{II}(x,t)$:

$$B_{II} = \rho_{II}\, A_{II} = \frac{\beta_{II}\, e^{\lambda_{II} \int \sqrt{\tau_{II}}\, dt}}{\{-2a_2 (x-a_3)\}^{\frac{1}{2}}} \tag{c.17}$$

$$\rho_{II} = \left\{ \frac{\gamma-1}{C_1} \left[(x-a_3)^2 \left(\frac{\lambda_{II}}{2\sqrt{\tau_{II}}} \frac{d\tau_{II}}{dt} - 2\lambda_{II}^2 \tau_{II} \right) + \right. \right. \tag{c.18}$$

$$\left. \left. + \frac{2}{3} \left(\frac{-a_2}{2} \right)^{\frac{3}{2}} \frac{\alpha_{II}}{a_2^3} (x-a_3)^{\frac{3}{2}} \left(\frac{1}{\sqrt{\tau_{II}}} \frac{d\tau_{II}}{dt} - 6\lambda_{II} \tau_{II} \right) + \frac{\alpha_{II}^2}{4a_2^3} \tau_{II} x - K_5 \right] \right\}^{\frac{1}{\gamma-1}}$$

$$A_{II} = \frac{\beta_{II}\, e^{\lambda_{II} \int \sqrt{\tau_{II}}\, dt}}{\{-2a_2 (x-a_3)\}^{\frac{1}{2}}} \{\rho_{II}^{-1}\} \tag{c.19}$$

$$u_{II} = \sqrt{\tau_{II}} \left\{ \frac{\alpha_{II}}{2a_2^2} \left[-2a_2 (x-a_3) \right]^{\frac{1}{2}} - 2\lambda_{II} (x-a_3) \right\} \tag{c.20}$$

D. SOLUTION OF THE BOUNDARY VALUE PROBLEM

For the inflow between hinged valves the initial and boundary conditions to be satisfied may be noted as:

$$
\left.
\begin{aligned}
&1.\ A(o,t) = A_{o,t} = A_{o,o} \\
&2.\ B(o,o) = \rho_s A_{o,o} \ (= \rho_s A_{o,t}) \\
&3.\ B(h,o) = \rho_s A_{h,o} \\
&4.\ B(h,t_1) = \mu\rho_s \nu A_{o,o} \\
&5.\ u(o,t) = f(t)
\end{aligned}
\right\} \quad (d.1)
$$

where

$$
\left.
\begin{aligned}
&A_{o,o} = A_{o,t} = 2kw \\
&\rho_s \text{ is stagnation density} \\
&\mu \text{ and } \nu \text{ are factors less than one} \\
&f(t) \text{ is a given function of time} \\
\text{and} \quad &t_1 \text{ is the opening time of the valves (this value will be used later)}
\end{aligned}
\right\} \quad (d.2)
$$

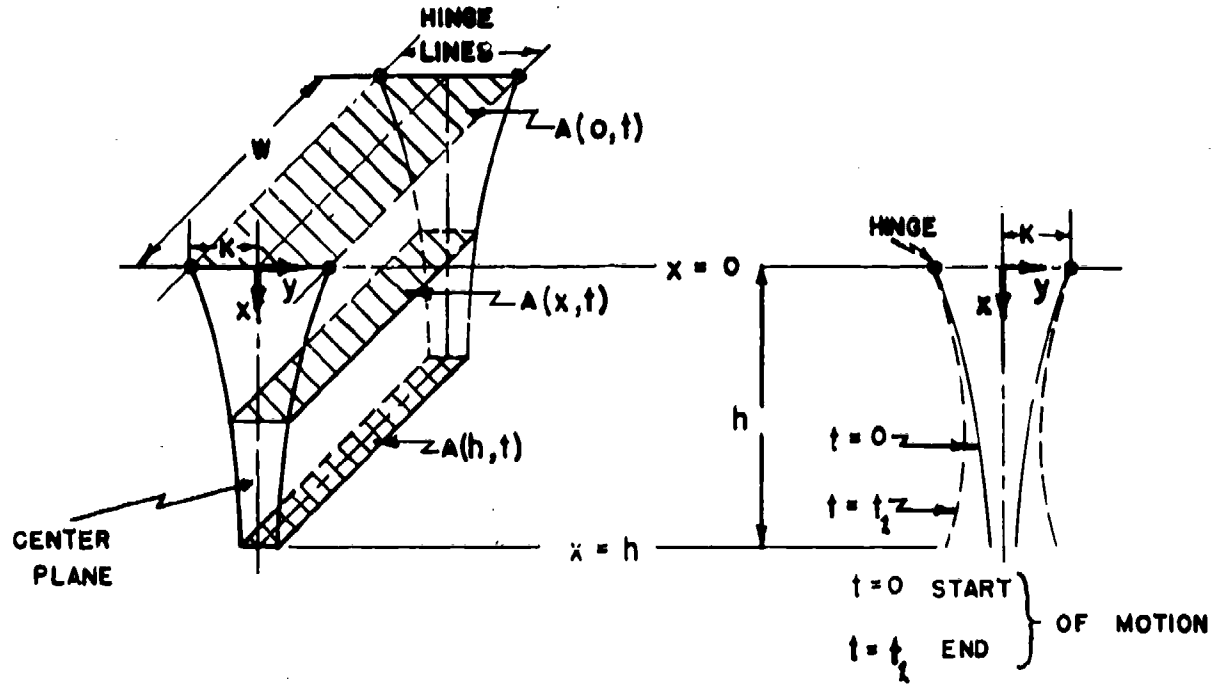

FIGURE 1

For *Case I.*, the arbitrary function of time $K_4(t)$ is determined from condition 1(d.1) to be:

$$K_4(t) = \frac{C_1}{\gamma-1}\left\{\frac{A_{o,o}}{\beta_I b} e^{\frac{1}{\lambda_I^2}\int\sqrt{\tau_I}\,dt}\right\} - \frac{\sqrt{\alpha_I}}{4c^3\sqrt{\tau_I}}\frac{d\tau_I}{dt} + \frac{\tau_I}{2c^3}\left\{\frac{\alpha_I}{4c} + \frac{\sqrt{\alpha_I}}{\lambda_I^2}\right\} \quad (d.3)$$

From condition 2(d.1) the product of the arbitrary constants b & β_I may be determined:

$$b\beta_I = A_{o,o}\,\rho_s\, e^{\frac{1}{\lambda_I^2}\left(\int\sqrt{\tau_I}\,dt\right)_o} \quad (d.4)$$

where $\left(\int\sqrt{\tau_I}\,dt\right)_o$ denotes the value of the integral at $t = 0$.

From condition 3(d.1) we obtain:

$$c = \frac{1}{h}\ln\left(\frac{A_{h,o}}{A_{o,o}}\right) \quad (d.5)$$

To find the unknown time function $\tau_I = \tau_I(t)$, the function $f(t)$ in condition 5(d.1) has to be chosen. Assuming that $f(t)$ can be approximated by a polynomial, i.e.:

$$u_I(o,t) = f(t) = b_o + b_1 t + b_2 t^2 \cdots = \sum_{n=o}^{n} b_n t^n \quad (d.6)$$

therefore from equation (c.15) τ_I is found to be:

$$\tau_I = \tau_I(t) = \frac{c^2 f(t)^2}{\left\{\frac{\sqrt{\alpha_I}}{2c} - \frac{1}{\lambda_I^2}\right\}^2} \quad (d.7)$$

Evaluating the following expressions:

$$\left.\begin{aligned} \int\sqrt{\tau_I}\,dt &= \frac{c f_1(t)}{\left\{\frac{\sqrt{\alpha_I}}{2c} + \frac{1}{\lambda_I^2}\right\}} \\ \text{where} \quad f_1(t) &= \left[b_0 t + b_1\frac{t^2}{2} + b_2\frac{t^3}{3} + \cdots\right] = \sum_{n=0}^{n}\frac{b_n t^{n+1}}{n+1} \end{aligned}\right\} \quad \text{(d.8)}$$

therefore at $t = 0$

$$\left(\int\sqrt{\tau_I}\,dt\right) = 0$$

and equation (d.4) reduces to:

$$b\beta_I = A_{o,o}\rho_s \qquad \text{(d.4a)}$$

$$\left.\begin{aligned} \frac{d\tau_I}{dt} &= \frac{2c^2 f(t) f_2(t)}{\left\{\frac{\sqrt{\alpha_I}}{2c} + \frac{1}{\lambda_I^2}\right\}^2} \\ \text{where} \quad f_2(t) &= \left[b_1 + 2b_2 t + 3b_3 t^2 + \cdots\right] = \sum_{n=1}^{n} n b_n t^{n-1} \end{aligned}\right\} \quad \text{(d.9)}$$

Using condition 4 (d.1) the constant α_I is determined:

$$\sqrt{\alpha_I} = \frac{2c}{\lambda_I^2}\left\{\frac{c\{f_1(t)\}_{t_1}}{ch - ln\mu\nu} - 1\right\}$$

denoting

$$\Delta_I = \frac{c\left(f_1(t)\right)_{t_1}}{ch - ln\mu\nu} \qquad \text{(d.10)}$$

the expression for α_I becomes:

$$\sqrt{\alpha_I} = \frac{2c}{\lambda_I^2}(\Delta_I - 1) \tag{d.11}$$

Inserting the values of the constants $b\beta_I$ (d.4a) and α_I (d.11) together with the arbitrary time functions $K_4(t)$ (d.3) and τ_I (d.7) in equations (c.13) (c.14), and (c.15) we obtain the following expressions to be used in the numerical calculations:

$$\rho_I = \left\{ \frac{\gamma-1}{C_1} \left[\frac{f_2(t)}{\Delta_I} \left(\frac{\Delta_I - 1}{c}(e^{-cx}-1) - x \right) - \frac{f(t)^2}{\Delta_I^2} \left(\frac{1}{2}(\Delta_I-1)^2 (e^{-2cx}-1) + (\Delta_I-1)(e^{-cx}-1) \right) + \frac{C_1}{\gamma-1} \rho_s^{\gamma-1} e^{\frac{1-\gamma}{\Delta_I} c f_1(t)} \right] \right\}^{\frac{1}{\gamma-1}} \tag{d.12}$$

$$A_I = A_{o,o}\, \rho_s\, e^{cx - c\frac{f_1(t)}{\Delta_I}} \left\{ \rho_I^{-1} \right\} \tag{d.13}$$

$$u_I = \frac{f(t)}{\Delta_I} \left\{ (\Delta_I - 1)\, e^{-cx} + 1 \right\} \tag{d.14}$$

Note: When values of $b\beta_I$ d.4a) and α_I (d.11) are substituted in equation (c.13), (c.14), and (c.15) as shown above, the arbitrary constant λ_I cancelled out of all the expressions.

For *Case II.*, the arbitrary function of time $K_5(t)$ is determined from condition 1 (d.1):

$$K_5(t) = \frac{1}{\gamma-1} \left\{ \frac{1}{\rho_{II}} \left[A_{o,o} (2a_2 a_3)^{\frac{1}{2}} e^{-\lambda_{II} \int \sqrt{\tau_{II}}\, dt} \right] \right\}^{1-\gamma} - \left\{ \frac{-2\lambda_{II}^2 \tau_{II}}{C_1} + \frac{\lambda_{II}}{2C_1\sqrt{\tau_{II}}} \frac{d\tau_{II}}{dt} \right\} a_3^2 - \frac{2}{3} \left(-\frac{a_2}{2} \right)^{\frac{3}{2}} \left(-a_3 \right)^{\frac{3}{2}} \frac{\alpha_{II}}{C_1 a_2^3} \left[\frac{1}{\sqrt{\tau_{II}}} \frac{d\tau_{II}}{dt} - 6\lambda_{II} \tau_{II} \right] \tag{d.15}$$

From condition 2 (d.1) the arbitrary constant β_{II} may be determined in the form:

$$\beta_{II} = A_{o,o}\rho_s [2a_2 a_3]^{\frac{1}{2}} e^{-\lambda_{II}[\int\sqrt{\tau_{II}}dt]_o} \tag{d.16}$$

where, as in the preceeding case $[\int\sqrt{\tau_{II}}dt]_o$ denote the value of the integral at t=0.

From condition 3(d.1) the arbitrary constant a_3 becomes:

$$a_3 = \frac{h}{1-\left\{\frac{A_{o,o}}{A_{h,o}}\right\}^2} \tag{d.17}$$

Using the expression for $u_{II}(o,t)$ as before,

$$u_{II}(o,t) = \sum_{n=o}^{n} b_n t^n = F(t) \tag{d.18}$$

one obtains:

$$\tau_{II} = \frac{F(t)^2}{\left\{\frac{\alpha_{II}}{a_2}\left(\frac{a_3}{2a_2}\right)^{\frac{1}{2}} + 2\lambda_{II}a_3\right\}^2} \tag{d.19}$$

and denoting:

$$\left.\begin{aligned} \int\sqrt{\tau_{II}}\,dt &= \left\{\frac{\alpha_{II}}{a_2}\left(\frac{a_3}{2a_2}\right)^{\frac{1}{2}} + 2\lambda_{II}a_3\right\}^{-1} F_1(t) \\ \text{where} \quad F_1(t) &= \int\sum_{n=o}^{n} b_n t^n\,dt \end{aligned}\right\} \tag{d.20}$$

and therefore t=0

$$(\int\sqrt{\tau_{II}}dt)_o \equiv 0$$

and equation (d.16) reduces to:

$$\beta_{II} = A_{o,o}\rho_s [2a_2 a_3]^{\frac{1}{2}} \tag{d.16a}$$

$$\left.\begin{aligned} \frac{d\tau_{II}}{dt} &= 2\left[\frac{\alpha_{II}}{a_2}\left(\frac{a_3}{2a_2}\right)^{\frac{1}{2}} + 2\lambda_{II}a_3\right]^{-2} F_2(t) \\ \text{where} \quad F_2(t) &= \frac{d}{dt}\left[\sum_{n=0}^{n} b_n t^n\right] \end{aligned}\right\} \quad (d.21)$$

Using condition 4 (d.1) one can calculate:

$$\alpha_{II} = \lambda_{II}\, a_2 \left[\frac{a_3}{2a_2}\right]^{-\frac{1}{2}} \Delta_{II} \quad (d.22)$$

where

$$\Delta_{II} = \frac{[F_1(t)]_{t_1}}{ln\left[\mu\nu\left\{-\frac{h-a_3}{a_3}\right\}^{\frac{1}{2}}\right]} - 2a_3 \quad (d.23)$$

Inserting the values of the arbitrary constants β_{II} (d.16a) and α_{II} (d.22) together with the arbitrary time functions $K_3(t)$ (d.15) and τ_{II} (d.19) in equations (c.18), (c.19), and (c.20) we obtain the following expressions to be used in the numerical calculations:

(d.24)

$$\rho_{II} = \left\{ \frac{\gamma-1}{C_1}\left[\left(\frac{-2F(t)^2}{(\Delta_{II}+2a_3)^2} + \frac{F_2(t)}{\Delta_{II}+2a_3}\right)\left((x-a_3)^2 - a_3^2\right) - \right.\right.$$

$$- \frac{1}{3}\left(-\frac{1}{a_3}\right)^{\frac{1}{2}} \Delta_{II}\left(\frac{-6F(t)^2}{(\Delta_{II}+2a_3)^2} + \frac{2F_2(t)}{\Delta_{II}+2a_3}\right)\left((x-a_3)^{\frac{3}{2}} - (-a_3)^{\frac{3}{2}}\right) +$$

$$\left.\left. + \frac{\Delta_{II}^2 F(t)^2 x}{2a_3(\Delta_{II}+2a_3)^2} + \frac{C_1}{\gamma-1}\left(\rho_s^{\gamma-1} e^{(\gamma-1)F_1(t)(\Delta_{II}+2a_3)^{-1}}\right)\right]\right\}^{\frac{1}{\gamma-1}}$$

$$A_{II} = A_{o,o}\,\rho_s \left[\frac{-a_s}{(x-a_s)}\right]^{\frac{1}{2}} e^{\frac{F_1(t)}{\Delta_{II}+2a_s}} \left\{\rho_{II}^{-1}\right\} \qquad \text{(d.25)}$$

$$u_{II} = F(t) \left[\frac{\Delta_{II}\left\{-\frac{x-a_s}{a_s}\right\}^{\frac{1}{2}} - 2(x-a_s)}{\Delta_{II} + 2a_s}\right] \qquad \text{(d.26)}$$

Note: When values of β_{II} (d.16a), α_{II} (d.22) are substituted in equations (d.12), (d.13) and (d.14), as shown above, the arbitrary constant λ_{II} cancelled out of all the expressions.

E. DETERMINATION OF THE MASS DISTRIBUTION OF THE REEDS

The differential equation for the forced vibration of a reed is

$$\frac{\partial^2}{\partial x^2}\left[EI\,\frac{\partial^2 y}{\partial x^2}\right] + m\,\frac{\partial^2 y}{\partial t^2} = q(x,t) \qquad \text{(e.1)}$$

where

E is the modulus of elasicity (lb/in^2)
I is the moment of inertia (in^4)
m is the mass of the reed per unit length $\frac{lbs.\ sec^2}{in^2}$
q is the resultant pressure force of pressures acting on both sides of reed (lb-in)

(e.2)

Inasmuch as the equilibrium equation (e.1) was used for small elements of the reed over which the moment of inertia was considered constant, equation (e.1) may be written:

$$EI\,\frac{\partial^4 y}{\partial x^4} + m\,\frac{\partial^2 y}{\partial t^2} = q(x,t) \qquad \text{(e.1a)}$$

In equation (e.1a) the right hand side (the forcing function) consists of:

$$q(x,t) = q_i(x,t) - q_{cc}(x,t) \qquad \text{(e.3)}$$

where

q_i is the pressure force on the inflow side of the reeds (lb/in)

q_{cc} is the pressure force on the combustion chamber side of the reeds (lb/in)

(e.4)

Therefore, equation (e.1a) may be written:

$$q_{cc}(x,t) = q_i(x,t) + EI \frac{\partial^4 y}{\partial x^4} - m \frac{\partial^2 y}{\partial t^2} \qquad \text{(e.1b)}$$

where

$EI \frac{\partial^4 y}{\partial x^4}$ is the bending force per unit length (lb/in)

$m \frac{\partial^2 y}{\partial t^2}$ is the inertia force per unit length (lb /in)

(e.5)

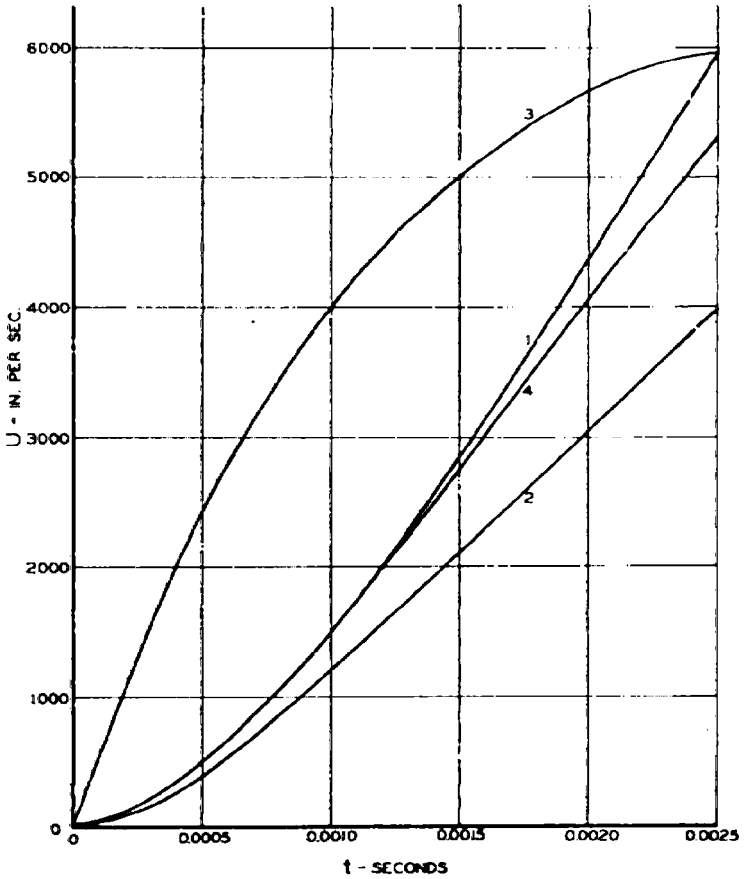

FIGURE 2

PRESCRIBED INFLOW-VELOCITY DISTRIBUTION AT THE ENTRANCE OF THE VALVES

1. and 3. Case I, area ratio 3:1
2. Case I, area ratio 5:1
4. Case II, area ratio 3.33:1

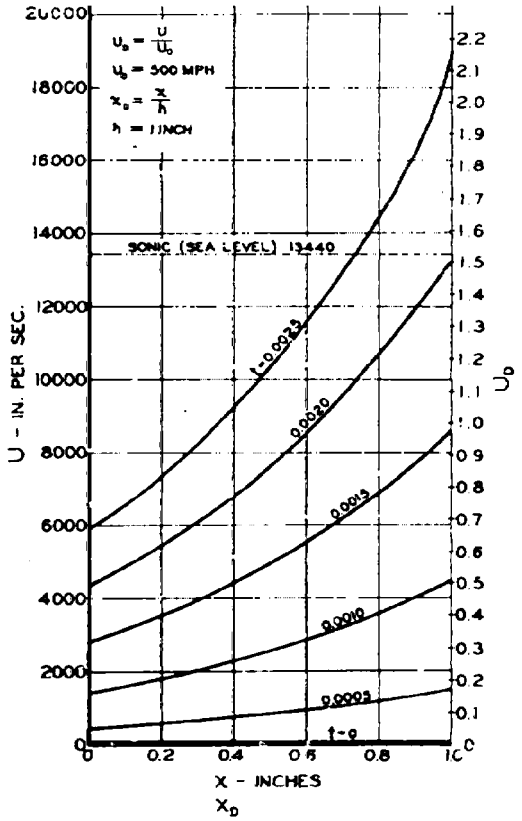

FIGURE 3

VELOCITY VARIATION DURING INFLOW AT VARIOUS TIMES

Case I, area ratio 3:1, corresponding to curve 1, Fig. 2.

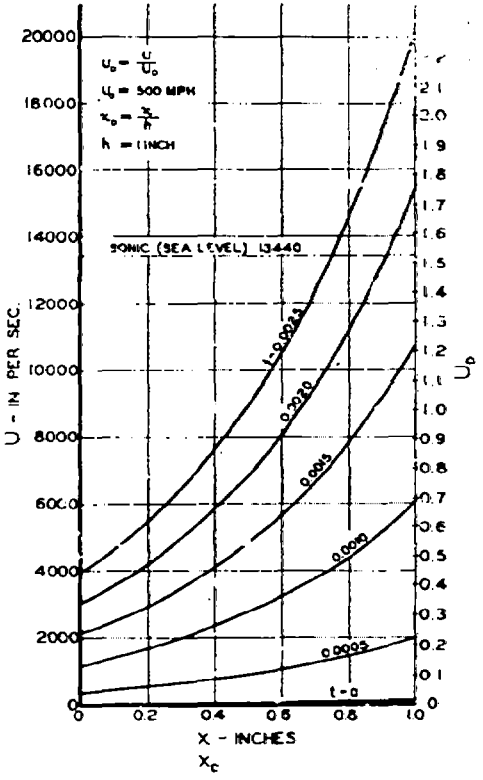

FIGURE 4

VELOCITY VARIATION DURING INFLOW AT VARIOUS TIMES.

Case I, area ratio 5:1, corresponding to curve 2, Fig. 2.

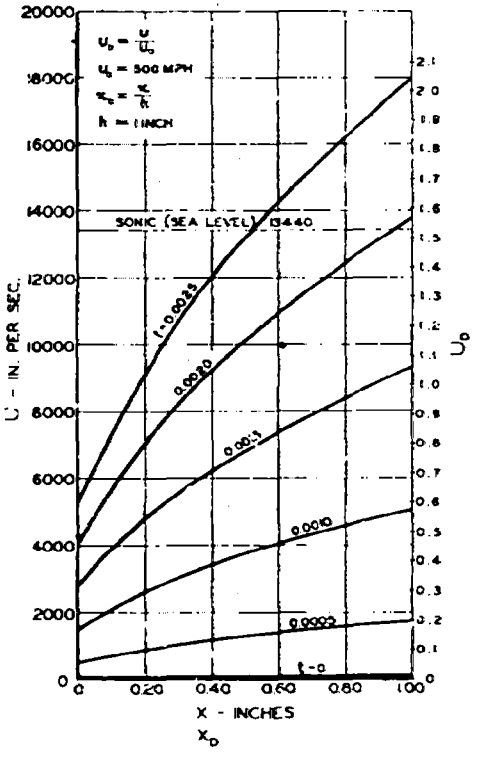

FIGURE 5

VELOCITY VARIATION DURING INFLOW AT VARIOUS TIMES.

Case I, area ratio 3:1, corresponding to curve 3, Fig. 2.

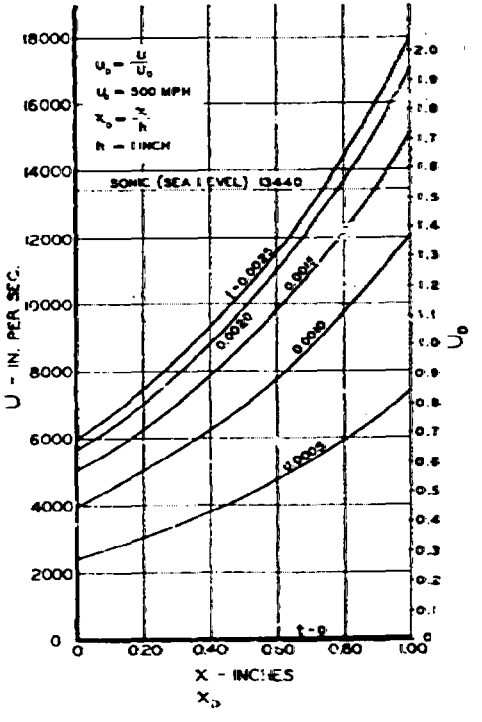

FIGURE 6

VELOCITY VARIATION DURING INFLOW AT VARIOUS TIMES.

Case II, area ratio 3.33:1, corresponding to curve 4, Fig. 2.

FIGURE 7

VALVE SHAPES AT THE START AND AT THE END OF INFLOW

1. *Case I, area ratio 3:1, corresponding to curve 1, Fig. 2.*
2. *Case I, area ratio 5:1, corresponding to curve 2, Fig. 2.*
3. *Case I, area ratio 3:1, corresponding to curve 3, Fig. 2.*
4. *Case II; area ratio 3.33:1, corresponding to curve 4, Fig. 2.*

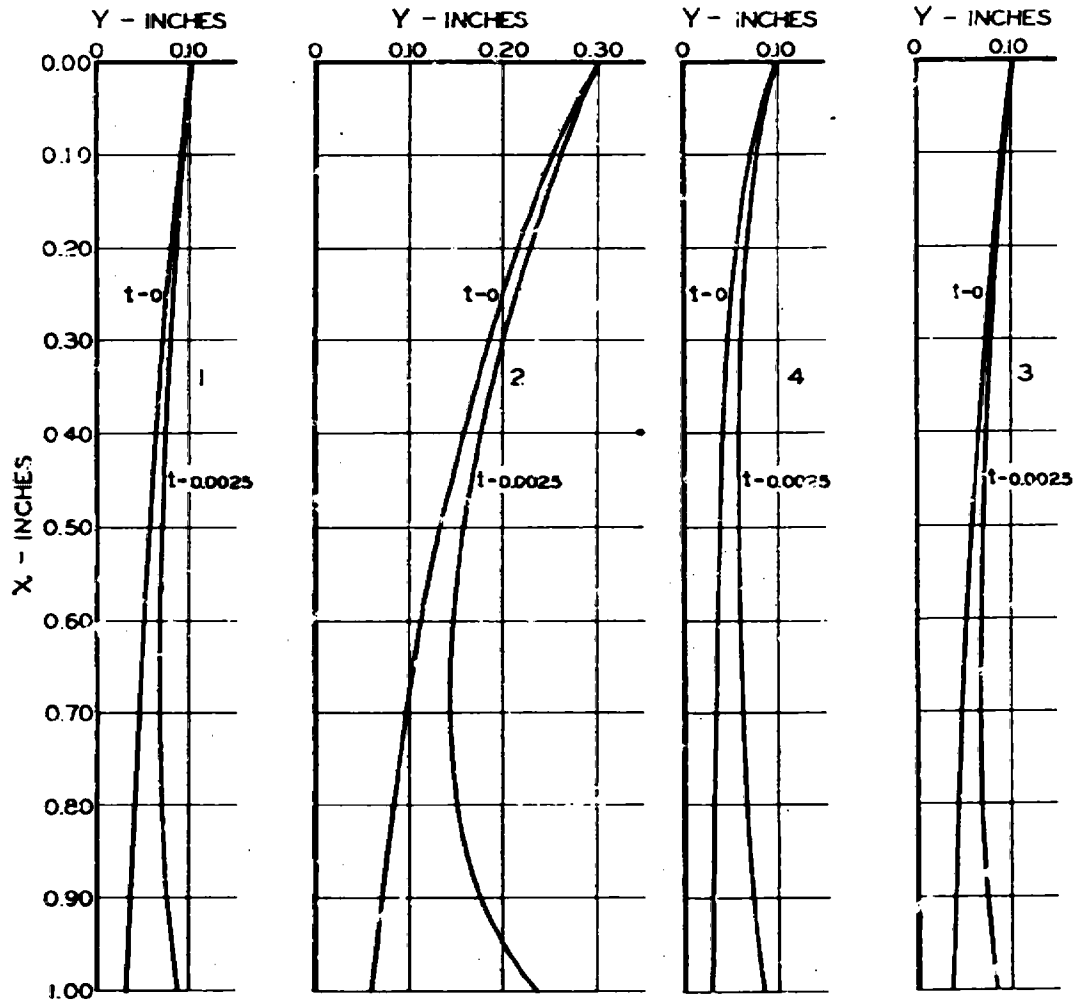

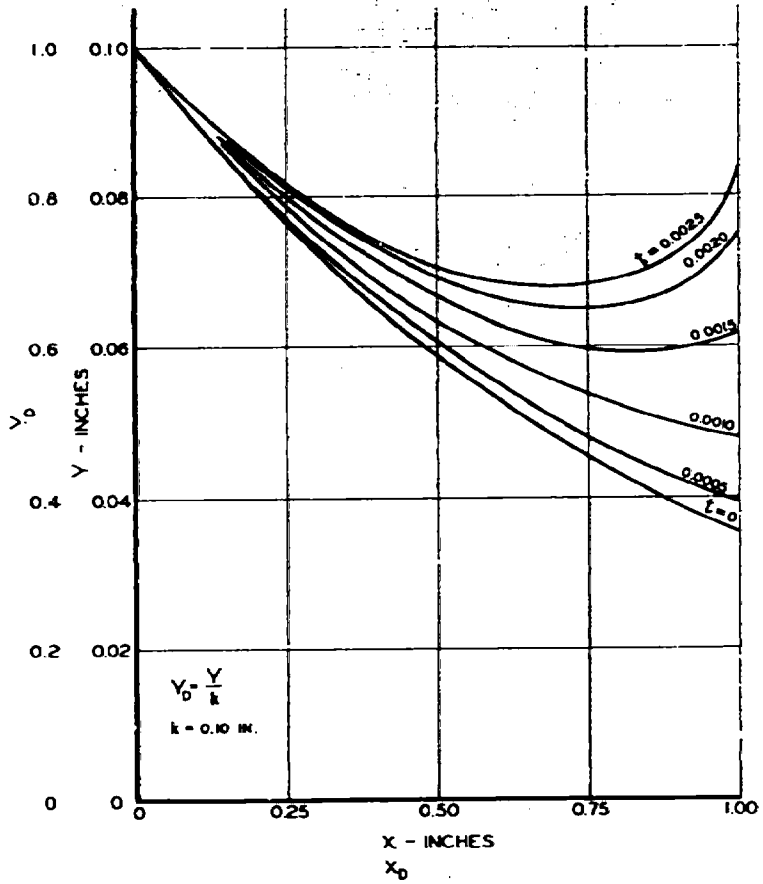

FIGURE 8

REED MOVEMENT

Case I, area ratio 3:1, corresponding to curve 1, Fig. 7.

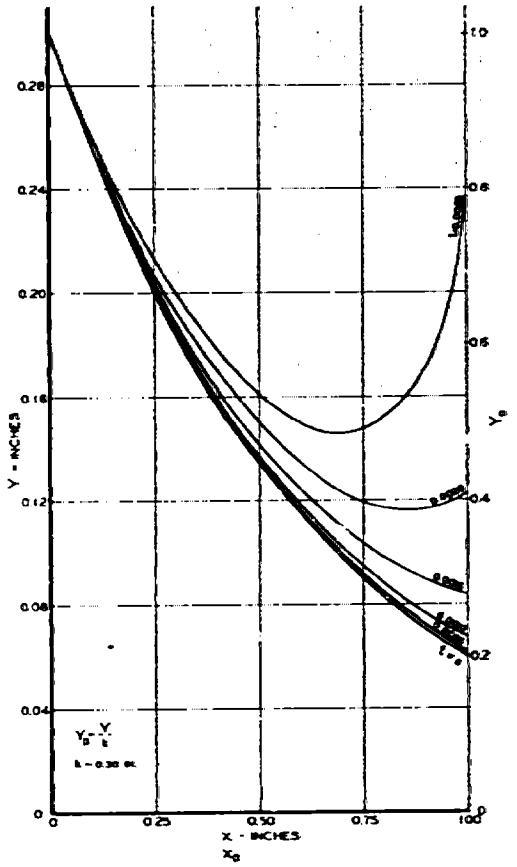

FIGURE 9

REED MOVEMENT

Case I, area ratio 5:1, corresponding to curve 2, Fig. 7.

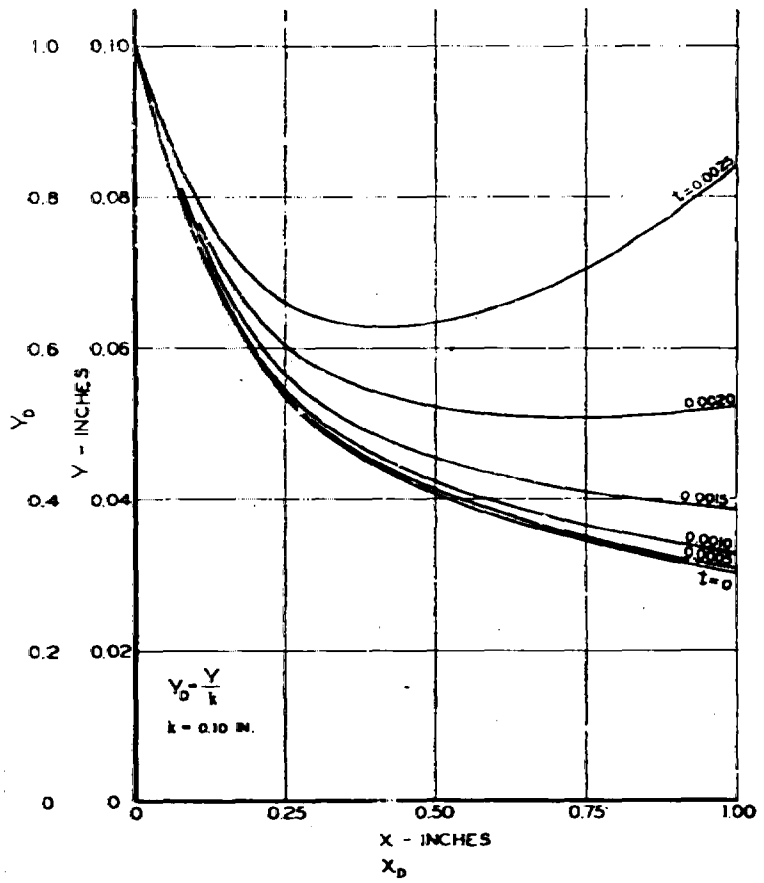

FIGURE 10

REED MOVEMENT

Case II, area ratio 3.33:1, corresponding to curve 4, Fig. 7.

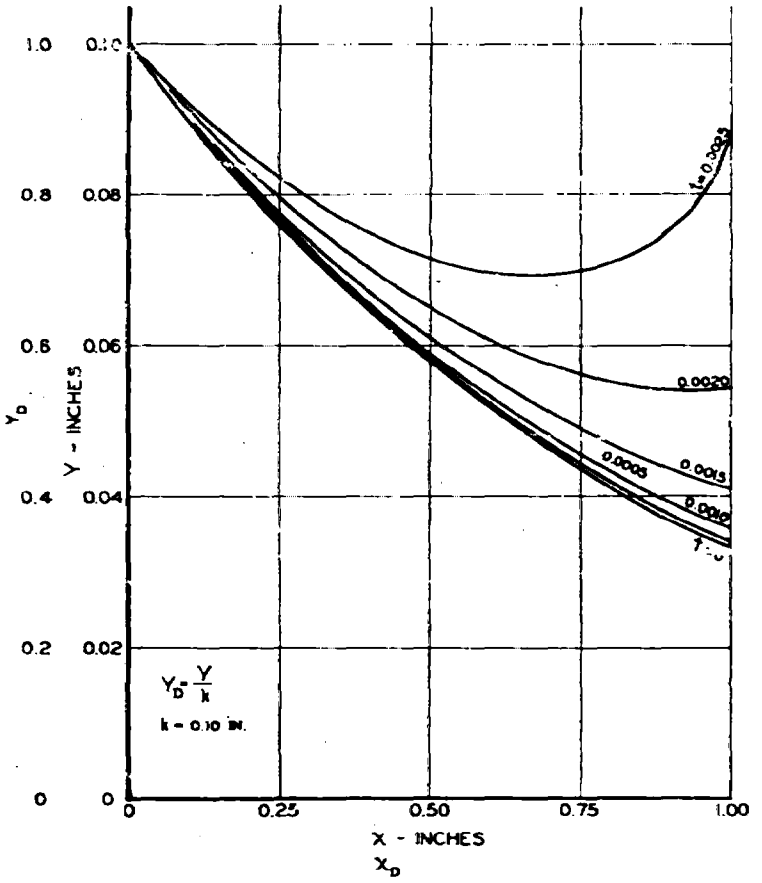

FIGURE 11

REED MOVEMENT

Case I, area ratio 3:1, corresponding to curve 3, Fig. 7.

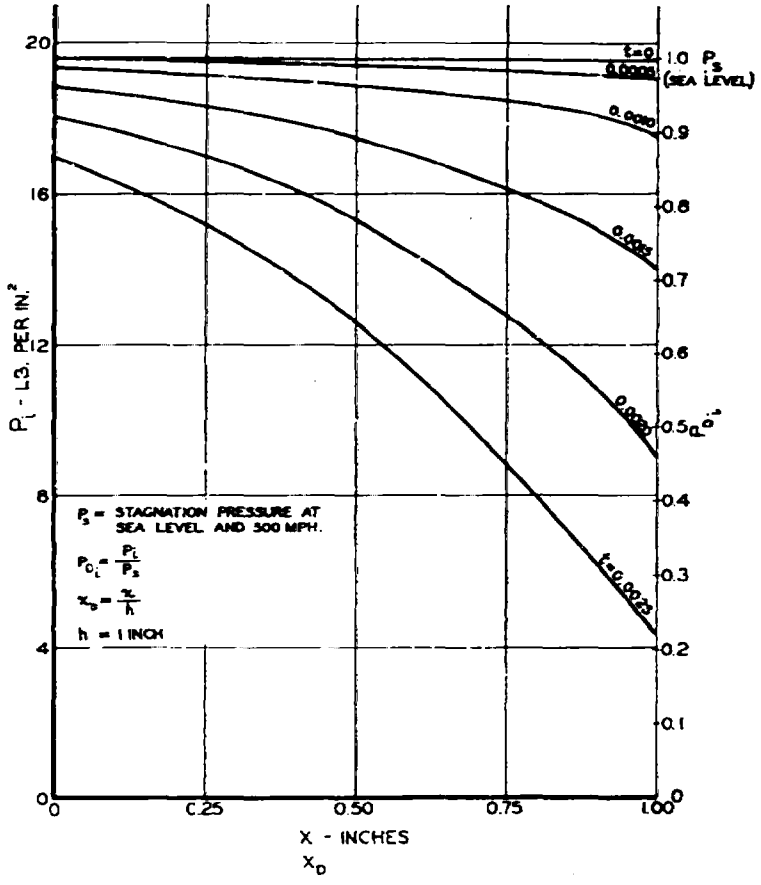

FIGURE 12

PRESSURE VARIATION ON THE INTAKE SIDE OF THE REEDS AT VARIOUS TIMES.

Case I, area ratio 3:1, corresponding to curve 1, Fig. 7.

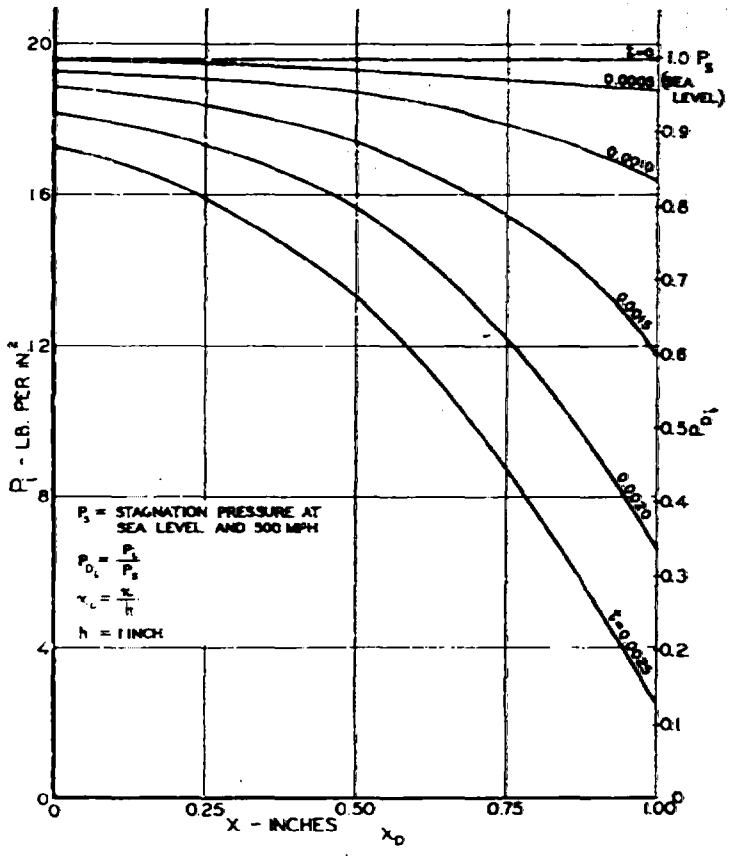

FIGURE 13

PRESSURE VARIATION ON THE INTAKE SIDE OF THE REEDS AT VARIOUS TIMES.

Case I, area ratio 5:1, corresponding to curve 2, Fig. 7.

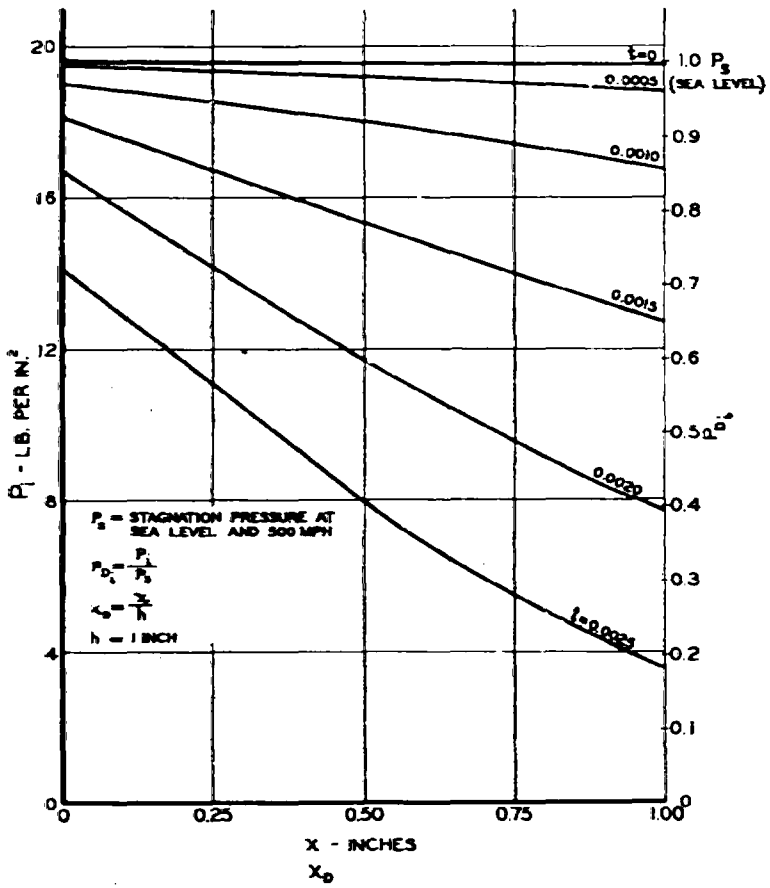

FIGURE 14

PRESSURE VARIATION ON THE INTAKE SIDE OF THE REEDS AT VARIOUS TIMES

Case II, area ratio 3.33:1, corresponding to curve 4, Fig. 7.

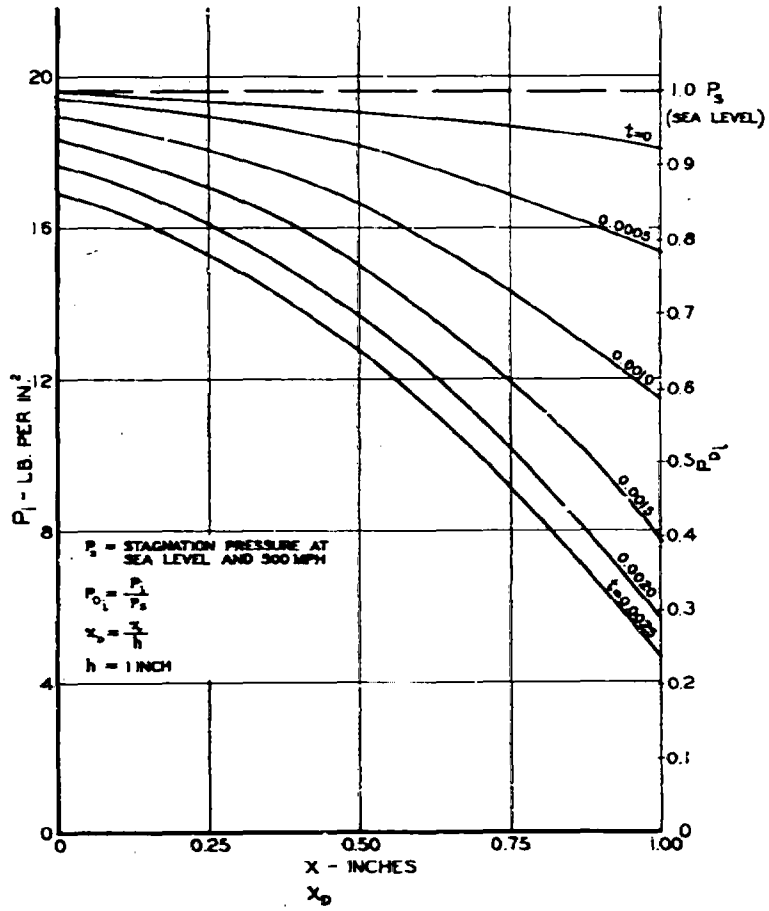

FIGURE 15

PRESSURE VARIATION ON THE INTAKE SIDE OF THE REEDS AT VARIOUS TIMES

Case I, area ratio 3:1, corresponding to curve 3, Fig. 7.

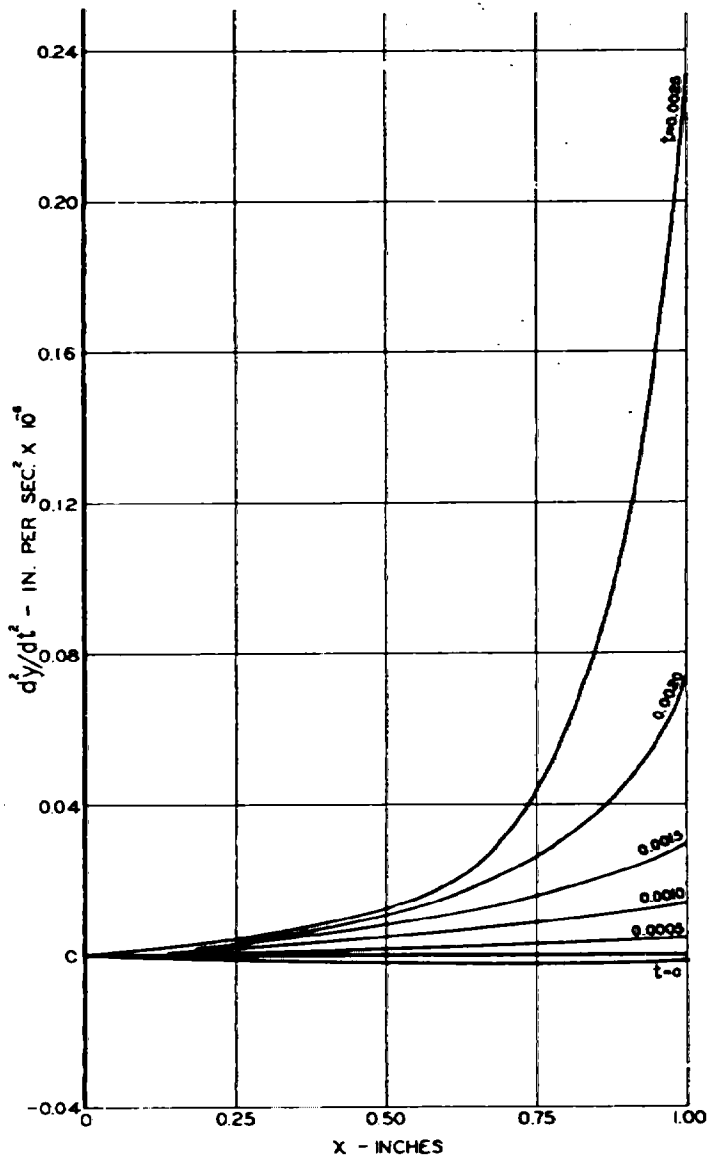

FIGURE 16

Case I, area ratio 3:1, corresponding to curve 1, Fig. 7.

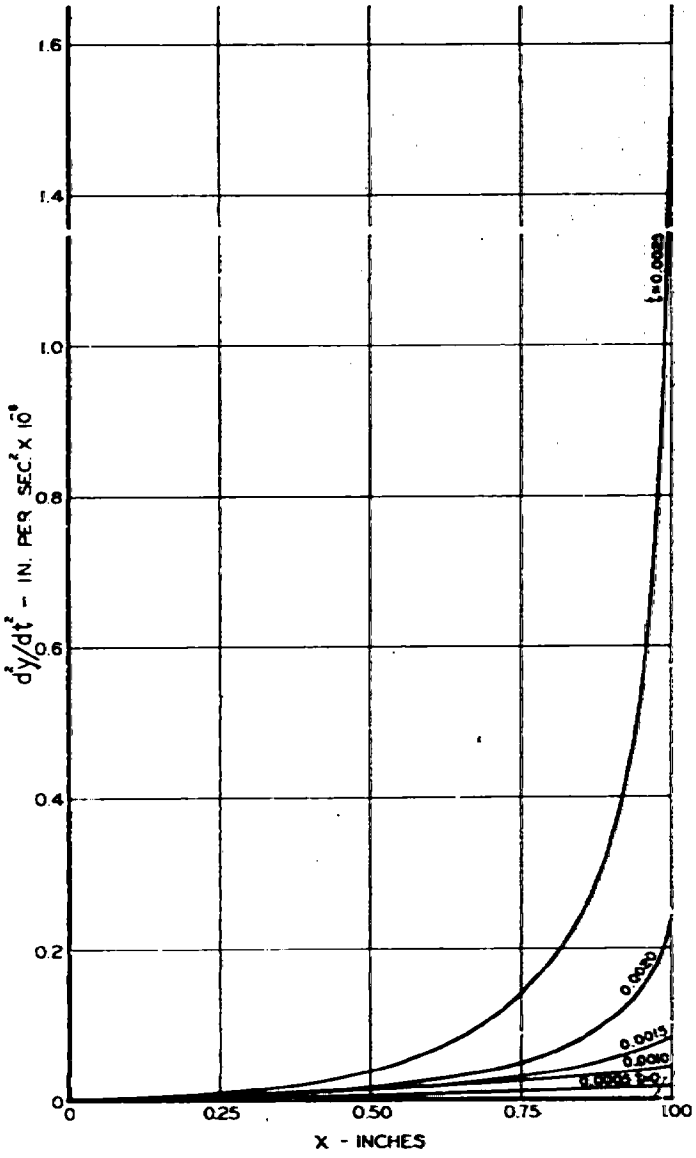

FIGURE 17

Case I, area ratio 5:1, corresponding to curve 2, Fig. 7.

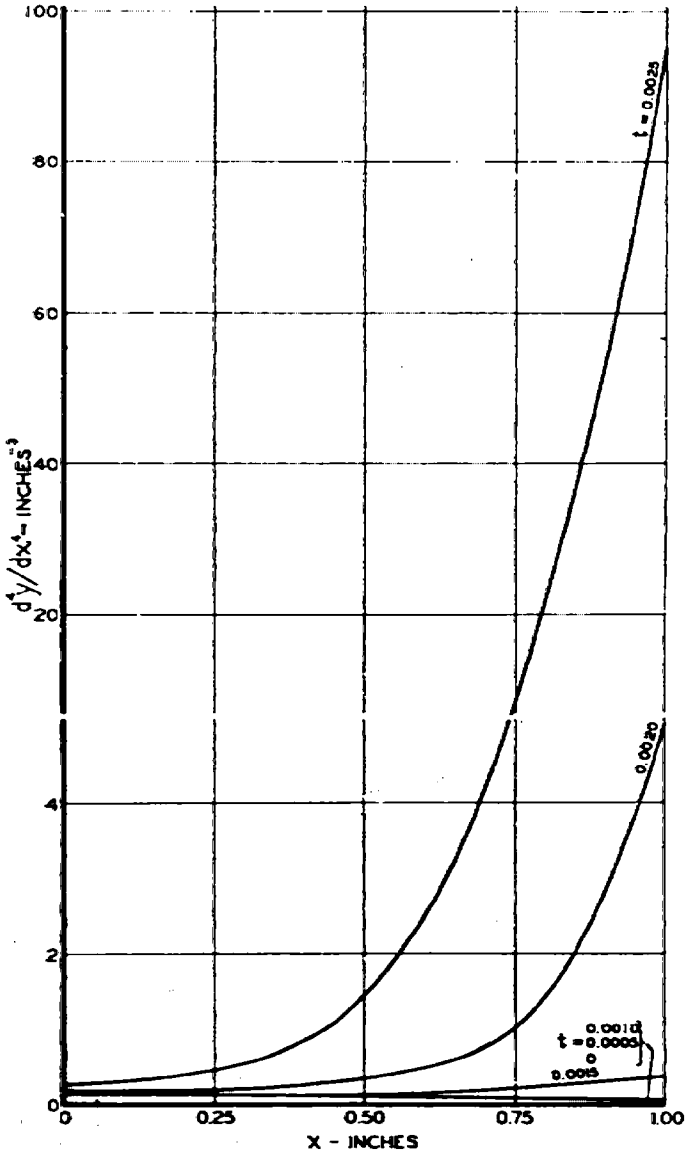

FIGURE 18

Case I, area ratio 3:1, corresponding to curve 1, Fig. 7.

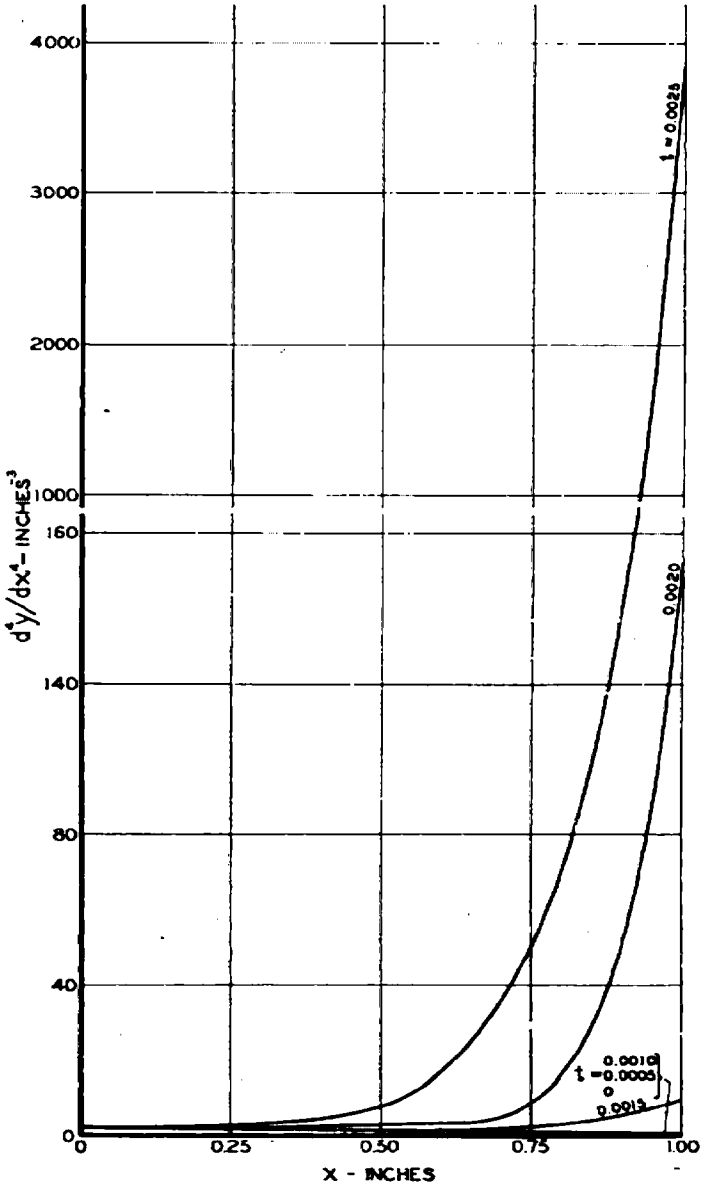

FIGURE 19

Case I, area ratio 5:1, corresponding to curve 2, Fig. 7.

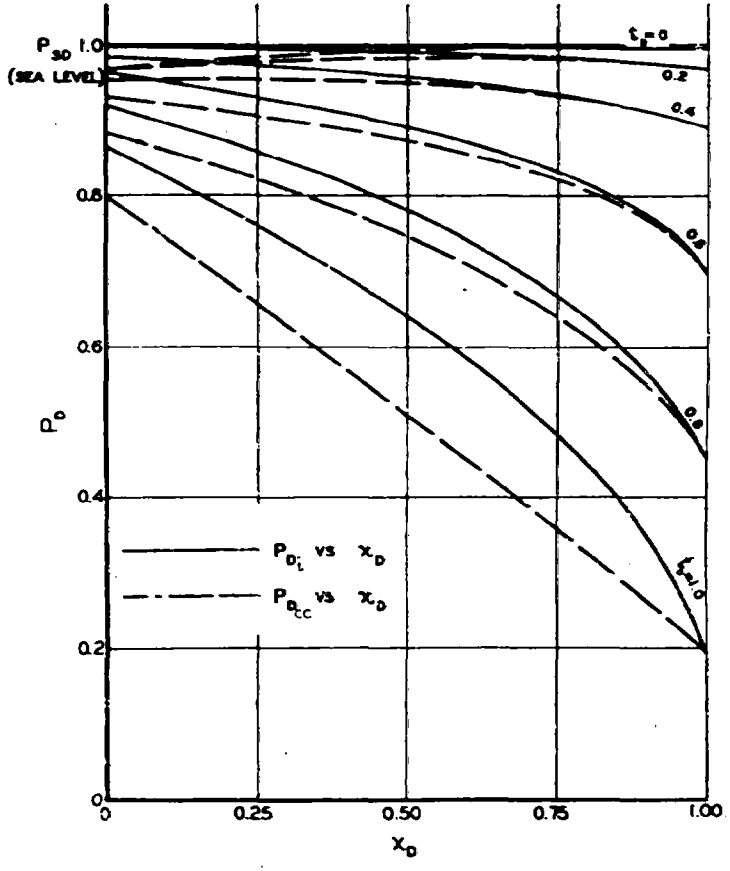

FIGURE 20

PRESSURE VARIATION ON BOTH SIDES OF THE REED

Case I, area ratio 3:1, corresponding to curve 1, Fig. 7.

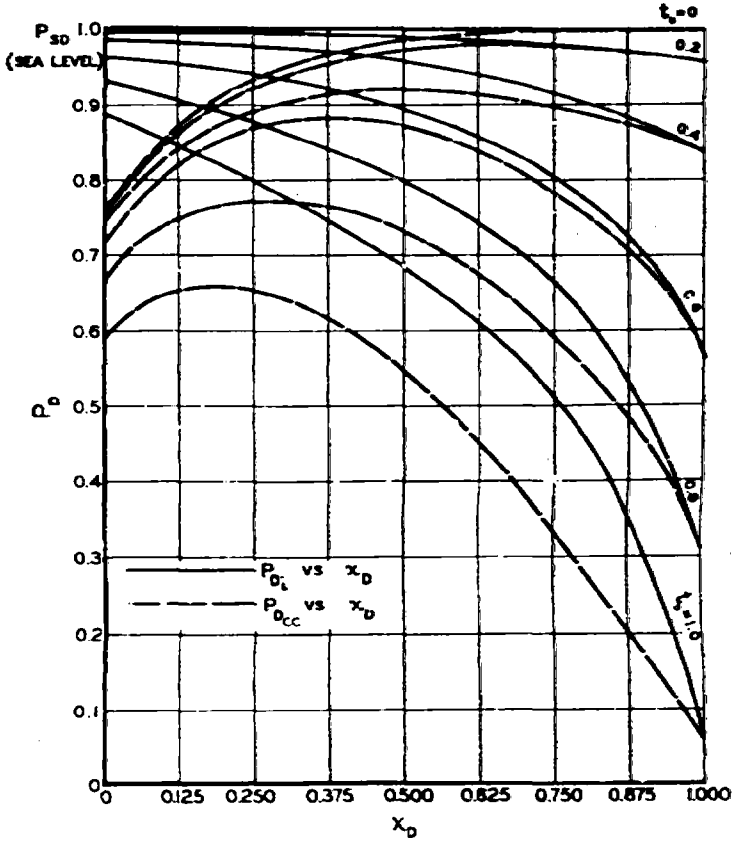

FIGURE 21

PRESSURE VARIATION ON BOTH SIDES OF THE REED

Case I, area ratio 5:1, corresponding to curve 2, Fig. 7.

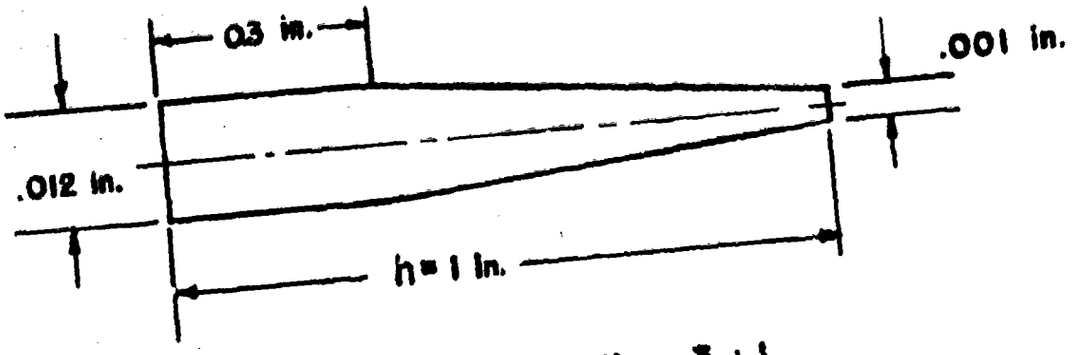

CASE I, Area ratio 5 : 1

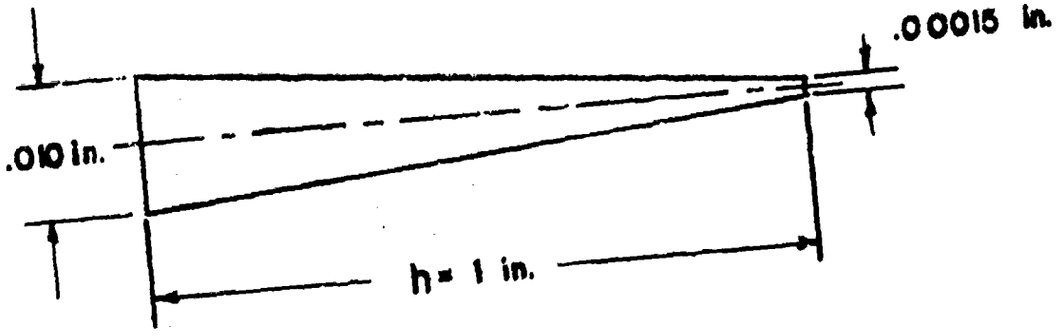

CASE II, Area ratio 5:1

FIGURE 22

MASS DISTRIBUTION OF REEDS FOR TWO EXAMPLES

TECHNICAL REPORT NO. 9 DISTRIBUTION LIST

1. Army-Navy-Air Force Guided Missiles List, Parts A,C,DP (List No. 8 dated 1 April 1949).
2. Policy Committee, Project Squid (6 copies).
3. Technical Representatives, Project Squid (7 copies).
4. Panel Members, Project Squid (10 copies).
5. Contract Administrators, Project Squid (9 copies).
6. Phase Leaders, Project Squid (2 copies).
7. Commanding Officer, Office of Naval Research, Chicago, Illinois.
8. Commanding Officer, Office of Naval Research, New York, New York.
9. Lt. Comdr. C. Hoffman, Bureau of Aeronautics, Power Plants Division, Experimental Engines Branch, Navy Department, Washington, D.C.
10. Comdr. J. L. Shoenhair, Office of Naval Research, Power Branch Naval Sciences Division, Washington, D.C.
11. Mr. Frank Tanczos, Guided Missiles Branch, Bureau of Ordnance, Navy Dept., Washington, D.C.
12. Mr. A.G. Leigh, Office of Naval Research Resident Representative, University of Rochester, Rochester, New York.
13. Guggenheim Aeronautical Laboratory, Pasadena, California, Attention: Professor Clark Millikan.
14. University of Minnesota, Chemistry Department, Minneapolis, Minnesota, Attention: Dr. B.L. Crawford.
15. Aeromarine Company, Vandalia, Ohio, Attention: Mr. William Tenney.
16. Department of Aeronautical Engineering, Johns Hopkins University, Baltimore, Maryland, Attention: Professor F. Clauser.
17. Columbia University Library, New York 27, New York.
18. Purdue University Library, Lafayette, Indiana, Attention: Mr. J. Moriarty.
19. Bodine Soundrive Company, Los Angeles, California, Attention: Mr. A. Bodine.
20. U.S. Navy Branch Office, San Francisco, California.
21. Officer in Charge, Naval Ordnance Test Center, Pasadena, California.
22. Department of Mechanical Engineering, University of California, Berkeley, California.
23. Commanding Officer, ONR Boston Branch Office, 495 Summer Street. (Navy Building) Boston 10, Massachusetts.
24. Commanding Officer, ONR Los Angeles Branch Office 1030 Green Street, Pasadena, California.
25. Office of Assistant Naval Attache for Research, Naval Attache, American Embassy, Navy 100, F.P.O, New York, N.Y.
26. University of Minnesota, Dept. of Aeronautical Engineering, Minneapolis 14, Minn., Attention: Professor J. D. Akerman.
27. Guggenheim Aeronautical Laboratory, California Institute of Technology, Pasadena, Calif., Attention: Dr. P. A. Lagerstrom.
28. University of California, Department of Engineering, Los Angeles 24, Calif., Attention: Dean L.N.K. Boelter.
29. Massachusetts Institute of Technology, Cambridge, Mass., Attention: Prof. J. H. Keenan.
30. Prof. A. R. Kantrowitz, Graduate School of Aeronautical Engineering, Cornell University, Ithaca, New York.